Journal of Energy Storage 136 (2025) 118439

Contents lists available at ScienceDirect

Journal of Energy Storage

journal homepage: www.elsevier.com/locate/est

Research papers

Techno-economic analysis of green hydrogen storage in salt caverns: Evaluating cycling effects and cavern scaling on the levelized cost of hydrogen storage in Ireland's power-to-X landscape

Ali Saberi Mehr [a,*], James G. Carton [b]

[a] School of Mechanical & Materials Engineering, University College Dublin (UCD), Dublin, Ireland
[b] School of Mechanical and Manufacturing Engineering, Dublin City, University (DCU), Dublin, Ireland

ARTICLE INFO

Keywords:
Green hydrogen
Large-scale storage
Salt cavern
Technoeconomic
Cycling
LCOH

ABSTRACT

This paper examines the techno-economic feasibility of utilising salt caverns for large-scale hydrogen storage in Ireland, leveraging wind energy and proton exchange membrane (PEM) electrolysers. The analysis focuses on optimising the integration of wind power with hydrogen production and storage, addressing key challenges such as energy curtailment, grid transmission constraints, and renewable energy intermittency. Findings highlight significant economic considerations, with a single hydrogen storage cavern requiring an initial investment of approximately €240 million, where geological site preparation and compressor systems constitute the largest cost components. Annual operational expenses (OPEX) are estimated at €4.6 million, largely due to compressor energy consumption and cooling requirements. The study emphasizes the critical impact of electrolyser scale on economic viability. Small-scale systems, such as a 20 MW PEM electrolyser, are economically unfeasible, with a levelised cost of hydrogen (LCOH) of around €10/kg and filling times extending up to 2.5 years. However, scaling up to a 200 MW PEM electrolyser dramatically improves cost efficiency, lowering the LCOH to approximately €0.83/kg and reducing filling times to just 90 days. This research provides a comprehensive framework for hydrogen storage development, offering key insights for policymakers and industry stakeholders to drive the renewable energy transition and enhance energy security through cost-effective and sustainable storage solutions.

Nomenclature

Symbol/Term	Description	Symbol/Term	Description
AFUDC	Allowance for Funds Used During Construction	PEM	Proton Exchange Membrane
CAPEX	Capital Expenditure	PEMCC	PEM Electrolyser Capital Cost
CC	Construction & Insurance Cost	Pinj	Injection pressure
CGS	Cushion Gas Cost	Pmax	Maximum storage pressure
CPC	Compressor Purchased Cost	Pmin	Minimum storage pressure
CUC	Compressor Unit Cost	SPCC	Surface Piping Capital Cost
Cpipe/km	Pipeline cost per km	SPIC	Surface Hydrogen Piping Infrastructure Cost
DMAX	Maximum Diameter of Salt Cavern	TDCC	Total Direct Capital Cost

(continued on next column)

(continued)

Symbol/Term	Description	Symbol/Term	Description
DMAX	Maximum cavern diameter	TFOM	Total Fixed Operation and Maintenance Cost
EEC	Electrical Equipment Cost	THST	Temporary Hydrogen Storage Tank Cost
ES	Engineering & Supervision Cost	TVOM	Total Variable Operation and Maintenance Cost
FCI	Fixed Capital Investment	TWh	Terawatt-hour
GFC	Geologic Formation Site Cost	V	Volume of cavern
GHG	Greenhouse Gas	VV	Void Volume of the Salt Cavern
GHPS	Grid-Interacted Hydrogen Production System	WIC	Well Implementation Cost
H	Cavern height	kWh	Kilowatt-hour
LCOH	Levelised Cost of Hydrogen	$\dot{m}$	Mass flow rate of hydrogen

(continued on next page)

* Corresponding author at: School of Mechanical & Materials Engineering, University College Dublin (UCD), Dublin, Ireland
E-mail address: ali.saberimehr@ucd.ie (A. Saberi Mehr).

https://doi.org/10.1016/j.est.2025.118439
Received 8 February 2025; Received in revised form 17 June 2025; Accepted 7 September 2025
Available online 15 September 2025

(continued)

LRD	Licensing, Research & Development Cost	g_f	Fracturing Gradient
Lpipe	Pipeline length	ηelec	Electrolyser efficiency
MDCC	Monitoring Device Capital Cost	ρCG	Density of cushion gas at 90 bar, 327.8 K
MMV	Measurement, Monitoring, and Verification	ρH2	Density of hydrogen at standard conditions
NMR	Nuclear Magnetic Resonance		
OPEX	Operating Expenditure		

1. Introduction

Undeniably, the prioritisation of the energy transition from fossil fuels to renewables is crucial for the survival of our planet. In this context, the demand for wind power, whether onshore or offshore, is experiencing a remarkable surge due to its potential to address both environmental and energy crises. As evidence of this, global installed wind power capacity reached nearly 850 GW by the end of 2021, including a new offshore wind power record of nearly 60 GW [1].

While wind power is key to decarbonising electricity, it faces limitations such as grid constraints, curtailment, and infrastructure challenges. A broader approach that integrates multiple renewable technologies and energy efficiency measures is essential to achieving a sustainable, low-carbon future [2,3]. The successful integration of wind turbines and electrolysers has been demonstrated, especially in situations where curtailment poses a significant challenge [4,5]. The utilisation of wind power to produce green hydrogen represents a significant stride forward in the energy transition. This is because hydrogen and its vectors have the potential to address demanding sectors that are challenging to decarbonise, such as goods vehicles, aircraft, and marine vessels, as well as industrial heating. However, it is important to recognise that hydrogen production is just the initial step in the hydrogen value chain. The subsequent stages, including transportation and storage, play a critical role and must be carefully considered.

To better position hydrogen within the broader energy storage landscape, it is essential to compare it with alternative storage technologies in terms of energy density, scalability, storage duration, and economic viability. While battery storage systems are well-suited for short-duration applications due to their high round-trip efficiency, they remain limited by relatively low energy densities and high capital costs at scale. Similarly, compressed hydrogen tanks and liquid hydrogen provide higher gravimetric energy density but are constrained by infrastructure complexity and safety considerations. Recent developments in chemical carriers like ammonia and ammonia borane offer long-duration storage potential, albeit with additional processing and regeneration costs. In contrast, geological storage of hydrogen in salt caverns offers a unique advantage; it combines high gravimetric energy density with very low levelised storage costs and vast scalability potential for multi-TWh seasonal storage. Table 1 provides a comparison of these technologies, underscoring the strategic value of salt cavern hydrogen storage in enabling deep decarbonisation and grid flexibility.

Large-scale storage technologies include geological solutions to store large amounts of storable gas (natural gas, carbon dioxide, and/or hydrogen). Salt domes (solid and homogeneous bodies) or bedded salt deposits (salt halite found in shallower depth, 1–2 km underground) can provide an opportunity to build an artificial chamber called a salt cavern by drilling the ground to a depth of around 1000 m to 1500 m so that hydrogen with a pressure of up to 250 bar can be injected into the generated cavern to be stored for further [11]. Salt caverns currently account for approximately 8 % of global underground gas storage capacity [12]. While they have predominantly been used for natural gas, practical experience with hydrogen storage in salt caverns remains limited. However, the growing demand for hydrogen presents an opportunity to transition these facilities toward storing green hydrogen. Salt caverns offer several advantages over other hydrogen storage technologies, including high hydrogen purity upon withdrawal, lower levelized storage costs, and enhanced safety. These benefits position salt caverns as a promising solution for large-scale, long-duration hydrogen storage in a decarbonised energy system [13,14].

Several years ago, Taylor et al. [15] highlighted that the cost of hydrogen storage can vary significantly, ranging from 30 % to 300 % of the hydrogen cost, the variation depending on various factors such as technical considerations, political factors, geological conditions, and the maturity of the technology employed. In the past couple of decades, researchers have extensively explored the potential use of salt caverns for hydrogen storage in different regions and more concise costs are available. One such study conducted by Ozarslan [16] examined the feasibility of utilising a large-scale salt cavern, specifically the Tuz Golu cavern in Turkey, for hydrogen storage. The technical analysis revealed that the cavern had a storage volume of 12 × 630,000 m^3, allowing for the storage of 1000 million m^3 of hydrogen at a maximum pressure of 220 bar. The withdrawal rate was estimated to be 40 million m^3/day. Lord et al. [17] developed detailed cost functions to assess the capital investment, operating costs, and maintenance expenses associated with underground gas storage technologies, including salt caverns. By considering salt deposit maps in different locations across the United States (Houston, Detroit, Pittsburgh, and Los Angeles), they conducted technoeconomic modelling. For instance, in the case of Houston, the cavern had a void volume of approximately 580,000 m^3, with the capacity to store 4367 t of hydrogen as the working gas and 1871 t as the cushion gas. It is indicated that the unit cost of hydrogen storage could be as low as 1.6 $/kg.

Several European initiatives have explored underground hydrogen storage in salt caverns, demonstrating the growing interest in large-scale, dispatchable renewable energy solutions. The HyCAVmobil project in Germany [18], for example, is one of the first to test hydrogen storage in a salt cavern under real operating conditions, with a storage volume of 500 m^3 and a focus on refuelling applications for mobility. Other projects, such as Hystories [19] and Underground Sun Storage in

Table 1
Comparative analysis of hydrogen and energy storage technologies based on some key factors.

Storage Method	Gravimetric Energy Density (kWh/kg)	Volumetric Energy Density (kWh/L)	Storage Conditions	Scalability	Storage Duration
Liquid Hydrogen (LH_2) [6]	33.3	2.36	−253 °C, 1 atm	Medium (scale-limited by boil-off)	Medium (~weeks)
Compressed H_2 (700 bar)	~1.48	~0.83	700 bar, 15 °C	Low (transport scale)	Short (hours–days)
Ammonia (NH_3) [7]	~5.2	~3.6	25 °C, 8–10 bar	High	Long (months+)
Ammonia Borane (AB) [8]	~2.5	~2.26	Solid, ambient	Medium	Long (months)
Lithium-Ion Battery [9]	~0.711	~1.65	Ambient	Low to Medium	Short (hours–days)
Diesel Fuel	~12.7	~10.7	Ambient	High	Long (years)
Salt Cavern H_2 Storage [10]	33.3	~0.5	~250 bar, ~60 °C underground	Very High	Very Long (months–years)

Austria [20], have investigated the technical feasibility and modelling of hydrogen injection in various geological formations. Under the EU-funded project named “HyUnder,” Iordache et al. [21] specifically focused on the potential of salt caverns for underground hydrogen storage in Romania. They identified four potential locations (Ocna Mures, Targu Ocna, Ocnele Mari, and Cacica) for hydrogen storage and investigated the hydrogen demand bandwidth. However, the study did not provide detailed technical specifications or economic aspects. The HyUnder project conducted case studies in six countries (Germany, France, the UK, Spain, the Netherlands, and Romania) and compared the findings across these regions emphasising the importance of large scale storage mechanics.

In this context, large-scale energy storage, quantitively TWh energy storage, seems to be vital for decarbonisation and the energy security. Renewable sources like wind power are intermittent, requiring storage technologies to capture excess energy during peak production for later use during high demand or low generation periods [22]. Energy storage ensures reliable power supply, balances demand, and enhances grid stability. Large-scale hydrogen storage enables long-duration storage of surplus renewable energy via electrolysis, reducing curtailment and supporting system flexibility. Strategically placed facilities can meet regional needs and strengthen energy security, making hydrogen a key enabler in the transition to a low-carbon future.

1.1. Problem statement

Ireland’s 2020 Programme for Government set a target of 5 GW of installed offshore wind capacity by 2030—a goal reaffirmed in the Climate Action Plan 2021 and the updated 2024 Plan. Looking further ahead, Ireland aims to reach 20 GW by 2040 and at least 37 GW by 2050, despite a projected national electricity demand of only 6–7 GW. Simultaneously, the country has committed to sourcing up to 80 % of its electricity from renewables by 2030 [23]. While this ambitious growth in offshore wind represents a critical step toward decarbonisation, it also introduces significant technical and operational challenges. Without complementary investments in grid infrastructure and large-scale energy storage, a substantial portion of generated electricity may go unused due to curtailment, transmission constraints, and dispatch limitations. These barriers can undermine both the economic viability and environmental benefits of expanded renewable capacity [24]. To maximise the value of offshore wind and ensure system flexibility, grid upgrades must be paired with scalable, long-duration storage solutions. These technologies are vital to capturing excess electricity during periods of high generation and redistributing it when demand rises or renewable output falls.

In parallel, Ireland’s National Hydrogen Strategy [25] outlines the strategic role of hydrogen in decarbonising hard-to-electrify sectors such as heavy transport, industry, and international shipping. The Strategy forecasts domestic hydrogen demand to reach 4.6–39 TWh/year by 2050, potentially increasing to 74.6 TWh/year when accounting for export-oriented sectors. Meeting this demand will require not only production capacity but also robust storage infrastructure.

Fig. 1a illustrates the distribution of salt structures throughout Europe and highlights the regions characterised by significant salt abundance. With reference to this figure, it becomes evident that the northeast region of Ireland (Larne salt field, Belfast) holds immense potential as a “very salt-rich” area. Therefore, in the present study, it is assumed that Larne site would be used as the potential region for storing hydrogen underground.

IslandMagee Co., [26] based in Northern Ireland (see Fig. 1b), embarked on a project in 2015 to develop seven salt caverns at the Larne site. These caverns, with a combined capacity of approximately 1.4 TWh (capable of storing approximately 500 million m^3 of hydrogen), may serve as a significant energy storage facility.

To realise such a large-scale hydrogen storage project, a clear roadmap is essential—addressing both the supply of hydrogen and its delivery to end-users. This involves evaluating production methods like electrolysis, necessary infrastructure, and identifying key sectors that would benefit most from hydrogen use, such as industry, transport, and power generation. One promising application is using stored hydrogen in gas turbines for clean, flexible backup electricity generation, contributing to a resilient and low-carbon energy system.

1.2. Research gap and present work

While numerous studies have investigated the techno-economic and operational potential of hydrogen storage in salt caverns across Europe and globally most have focused on small-scale pilot systems, mobility applications, or generic regional assessments without integrating national energy system needs or specific geological characteristics. To date, there is limited research dedicated to Ireland-specific geological and policy contexts, despite the country’s ambitious offshore wind targets and emerging hydrogen strategy.

In particular, previous studies have not explored Ireland’s Larne salt

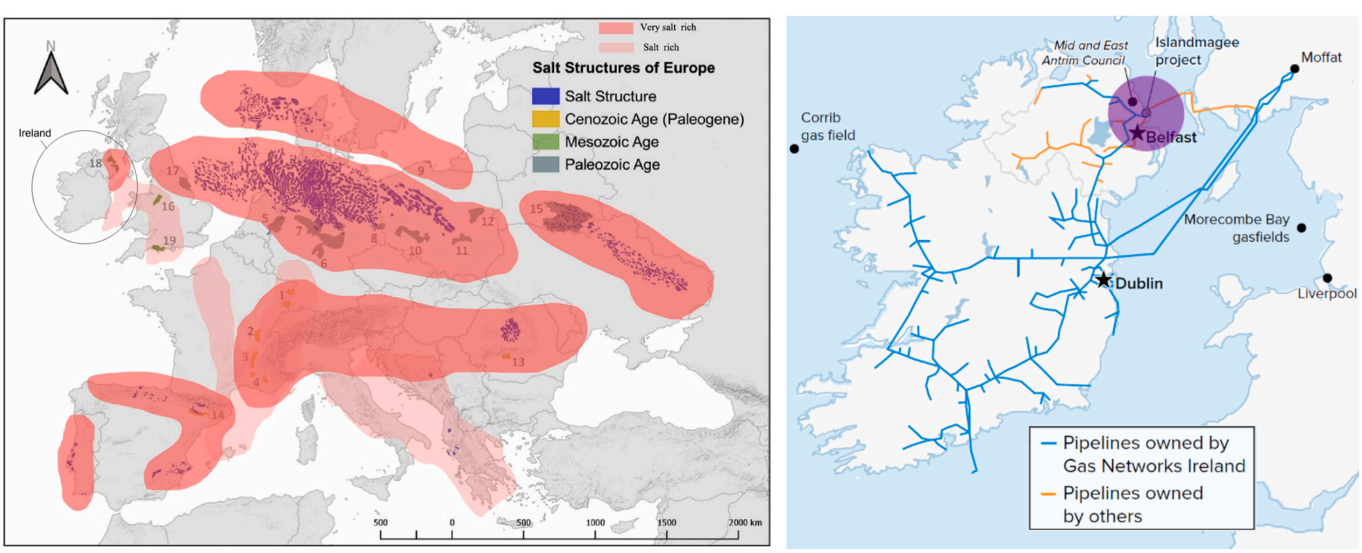

Fig. 1. a) Map of European salt deposits and salt structures including “salt rich” and “very salt rich” regions: modified version [13,27], b) Map of Ireland including Islandmagee proposed project located in Larne, Northern Ireland.

field as a strategically located, salt-rich formation capable of enabling multi-TWh scale hydrogen storage. Nor have they assessed its role in addressing seasonal grid balancing challenges or coupling hydrogen use with the country's decarbonisation goals in sectors such as industry and transport. Moreover, while the importance of hydrogen cycling has been recognised in earlier technical modelling efforts, the quantitative impact of cyclic injection and withdrawal on both performance metrics (e.g., cavern fill time, storage efficiency) and economic viability (CAPEX/ OPEX trade-offs) has not been extensively addressed in prior literature.

This study advances the state of the art in large-scale hydrogen storage by delivering a geographically specific techno-economic assessment focused on Ireland's Larne salt field—an underexplored, "very salt-rich" site identified for its substantial potential. By incorporating realistic wind profiles and using Ireland's policy targets as boundary conditions, the study offers a location-sensitive model that bridges the gap between national energy strategies and infrastructure-scale implementation.

In particular, the work introduces a novel evaluation of hydrogen injection and withdrawal cycling effects, a dimension often simplified or neglected in similar studies. Through detailed simulation and sensitivity analysis, it quantifies the impact of compressor sizing and cycling frequency on both the levelised cost of hydrogen (LCOH) storage and operational performance. This includes a breakdown of CAPEX and OPEX dynamics as a function of compressor configurations—highlighting the economic trade-offs that influence system optimisation.

2. Proposed system description

A schematic diagram of the proposed system is shown in Fig. 2. Leveraging the significant wind potential in Ireland, the power supply for the PEM electrolyser is sourced from the Rathsherry wind farm (see Fig. 4). The wind-generated power meets the energy requirements of the electrolyser, which produces hydrogen. This hydrogen is then compressed to the necessary pressure for underground storage in a salt cavern using a compressor. Initially, one hydrogen cavern will be established, with plans to progressively convert the remaining six caverns, currently designated for natural gas storage, to hydrogen storage. As illustrated, the produced hydrogen is subsequently extracted and utilised in a gas turbine unit operating in combined heat and power (CHP) mode to generate electricity and provide heating. Additionally, a valve in the system allows for the injection of hydrogen into the natural gas grid [28]. Although this blending is not accounted for in the modelling, it represents a promising future option. To ensure smooth operation of hydrogen storage in the salt cavern, an auxiliary hydrogen tank is included as a temporary small storage solution. This tank serves as a backup, storing and supplying hydrogen during periods of high demand or unforeseen circumstances. In the present work, the primary focus is on the storage aspect; therefore, as illustrated in Fig. 2, the scope of our research is limited to hydrogen production and storage.

Given Ireland's substantial electrical demand, wind power production is scaled up to match this demand. Initially, the model will be based on the chosen wind farm, with results recalculated for the scaled-up scenario. It is important to note that, based on the assumed wind farm, the hydrogen production would be minimal compared to the

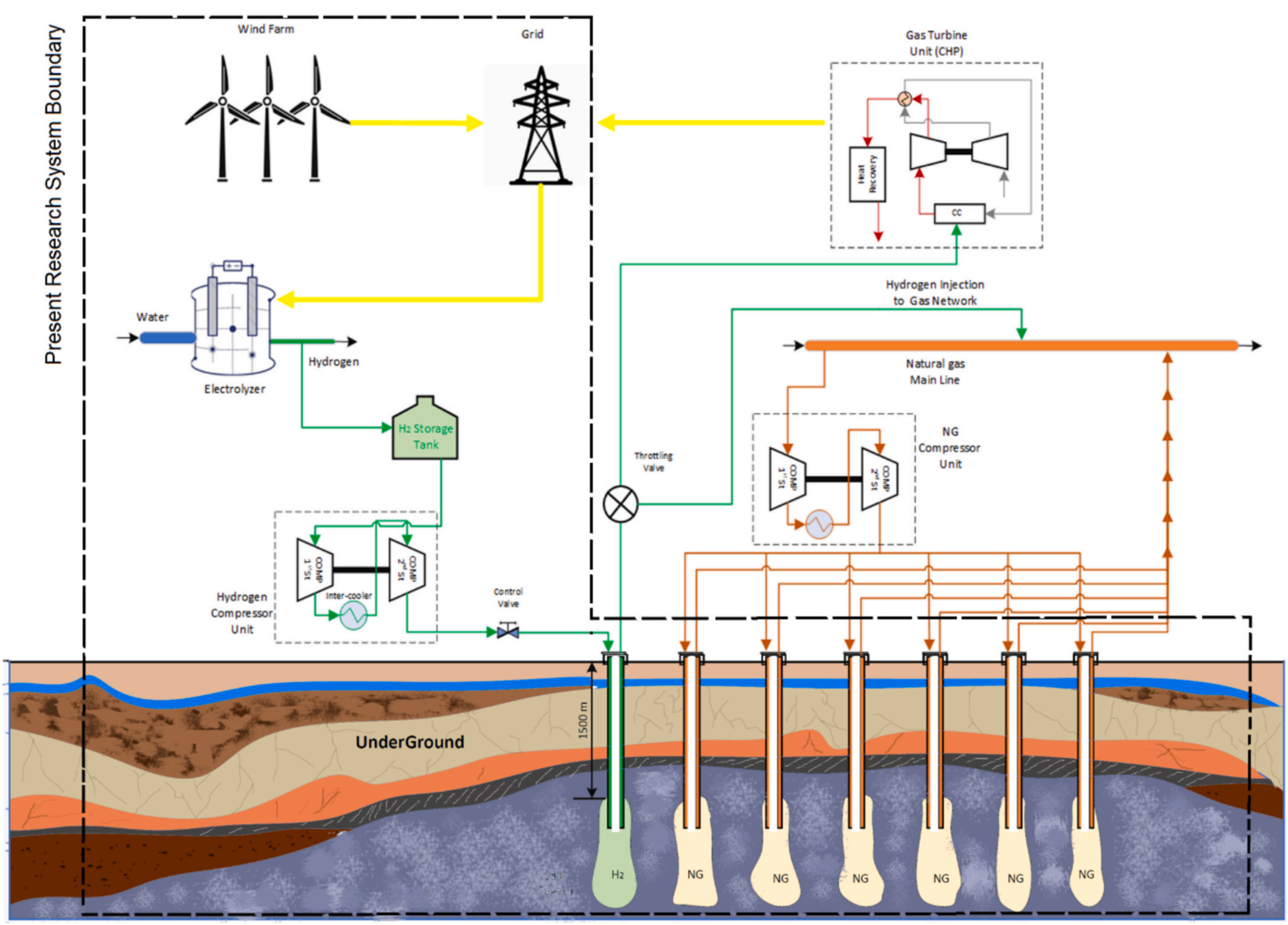

Fig. 2. Proposed configuration for utilisation of stored hydrogen in salt cavern by gas turbine unit.

capacity of a single cavern. However, this modelling approach allows for an initial analysis before adjusting to the scaled-up scenario.

3. Methodology

The proposed system consists of two main sections: hydrogen production, and storage in the promising salt caverns. In our modelling process, we have utilised inputs such as the capacity of the wind farm (with a nominal power of 21 MW) and specific weather data for Ireland (Fig. 3).

Furthermore, in the subsequent subsections, each section is comprehensively described in terms of the modelling methodologies employed. This detailed exploration delves into the specific approaches and techniques utilised to accurately capture and represent the intricacies of each section within the proposed system. By elucidating the modelling methodologies, a clearer understanding of the analysis and simulation techniques utilised in this study can be attained. This information serves to enhance the transparency and reproducibility of the research, enabling readers to grasp the systematic and rigorous approach undertaken in the modelling of each individual section.

3.1. Technical analysis

3.1.1. Hydrogen production (wind-PEM electrolyser)

In this section, using the wind power to produce green hydrogen is introduced. Thermodynamic modelling has been performed considering each component of the system as a separate control volume. To do so, the energy balance equation as well as general mass balance equations for all parts are applied as [29];

$$\sum_i \dot{m}_i = \sum_e \dot{m}_e \tag{1}$$

$$\dot{Q} + \sum_i \dot{m}_i \left(h_i + \frac{v_i^2}{2} + gz_i \right) = \sum_e \dot{m}_e \left(h_e + \frac{v_e^2}{2} + gz_e \right) + \dot{W} \tag{2}$$

Where, $\dot{m}$, $\dot{Q}$ and $\dot{W}$ are mass flow rate, the heat transfer rate crossing the control volume boundary and power (produced/consumed) for the component, respectively. Also, h is the enthalpy of the working fluid

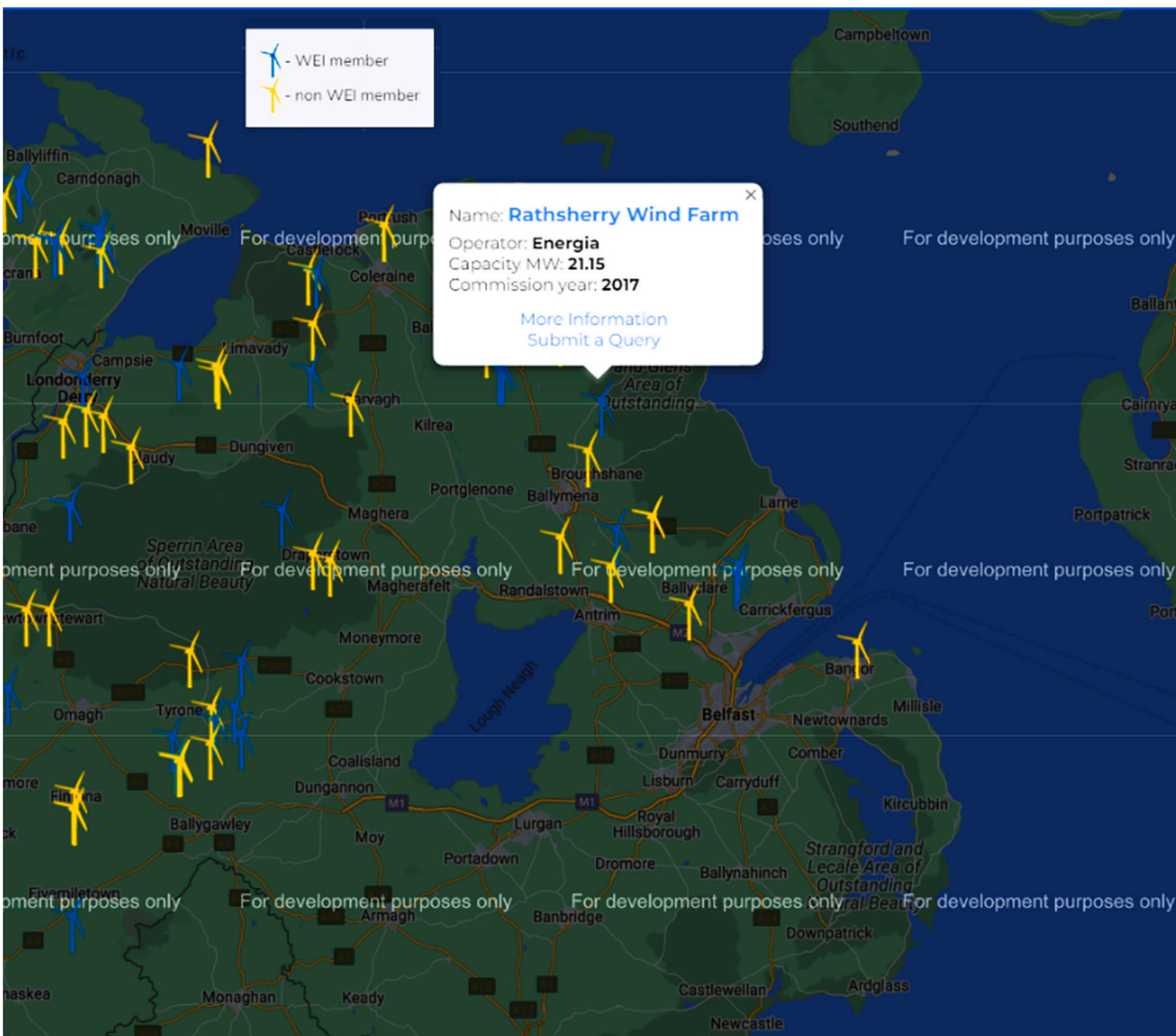

Fig. 3. Location and information of Rathsherry wind farm operated by Energeia in Northern Ireland, UK.

associated with each stream in the proposed system. Note that, $\frac{v^2}{2}$ and gz are the kinetic and potential energy of the working fluid, respectively.

To analyse wind power, data from the literature [30] were taken as illustrated in Fig. 3. This data serves as a reliable and representative source for studying the characteristics and availability of wind power during that specific period.

Furthermore, in line with the modelling of the electrolyser, it is essential to emphasise that the initial step involves calculating the energy required for the electrochemical process, disregarding any losses. This calculation serves as the foundation for understanding the energy demands of the electrolyser and allows for accurate modelling and analysis of the system's performance.

$$\Delta H = \Delta G + T\Delta S \tag{3}$$

In the above relation, ΔG ΔGis the required electrical energy which is calculated by Gibbs free energy. Also, the required thermal energy is $T\Delta S$ TΔSjoules per mole of hydrogen. From the thermodynamic tables, the required values and information such as G, H and S for hydrogen, oxygen and water can be extracted [31].

The molar flow rate of hydrogen produced in units of moles per second is obtained from the following equation:

$$\mathrm{N_{H2,out}} = \frac{\mathrm{J}}{2\mathrm{F}} = \mathrm{N_{H2O,reacted}} N_{H_2,out} = \frac{1}{2F} = N_{H_2O,reacted} \tag{4}$$

In the above equation, F is Faraday's constant coefficient. The flow rate of unreacted water and produced oxygen in the reaction is obtained through the following relations:

$$\mathrm{N_{O2,out}} = \frac{\mathrm{J}}{4\mathrm{F}} N_{O_2,out} = \frac{1}{4F} \tag{5}$$

$$N_{H_2,out} = N_{H_2,in} - \frac{1}{2F} \tag{6}$$

Using the definition of the input voltage to the electrolyser, the consumed electrical energy is obtained by the following relationship:

$$E_{electric} = JV \tag{7}$$

where, V represents the voltage of the electrolyser and is obtained by the following relation:

$$V = V_0 + V_{act,a} + V_{act,c} + V_{ohm} \tag{8}$$

The necessary details for the calculation of different electrolyser voltage statements are given in Table 1.

Table 1. Equations related to the calculation of voltage in the PEM electrolyser [32].

Nernst equation	$V_0 = 1.299 - 8.5 \times 10^{-4}(T_{PEME} - 298)$
Anode overpotential equation	$V_{act,a} = \frac{RT}{F}\sinh^{-1}\left(\frac{J}{2J_{0,a}}\right); J_{0,a} = J_0^{ref} e^{\frac{-E_{act,a}}{RT}}$
Cathode overpotential equation	$V_{act,c} = \frac{RT}{F}\sinh^{-1}\left(\frac{J}{2J_{0,c}}\right); J_{0,c} = J_0^{ref} e^{\frac{-E_{act,c}}{RT}}$
Ohmic overpotential equation	$V_{ohm} = J \times R_{PEME}; R_{PEME} = \int_0^D \frac{dx}{\sigma_{PEME}[\lambda(x)]}$ $\sigma_{PEME}[\lambda(x)] = [0.5139\lambda(x) - 0.326]e^{1268\left(\frac{1}{303} - \frac{1}{T_{PEME}}\right)}$ $\lambda(x) = \frac{\lambda_a - \lambda_c}{D}x + \lambda_c$

3.1.2. Hydrogen storage (salt cavern)

The size of a salt cavern is determined by its shape and dimensions, which are influenced by the thickness of the rock salt layer (Fig. 5). A typical design for a storage cavern involves a cylindrical shape as the main storage area, with a desired diameter D_{MAX}. The lower portion of the cavern is typically occupied by a conical incision, approximately 1/6 of the D_{MAX} height, while the upper part of the cavern is occupied by a dome shape that can be approximated as a cone, around 1/3 of the D_{MAX} height. Fig. 4 illustrates the simplified shape of a cavern, highlighting the cylindrical main storage section.

To assess the potential for hydrogen storage in rock salt, certain assumptions were made regarding the dimensions. Specifically, a safety pillar thickness of 55 m was assumed both at the top, W_{TP}, (50 m) and bottom, W_{BP}, (5 m) of the cavern, along with a minimum neck length, L_N, of 15 m. With these parameters in mind, the height of the cavern (H) for a given layer thickness (W) can be determined using the following relationship [33]:

$$H = W - (W_{TP} + W_{BP} + L_N) \tag{9}$$

The volume of such cavern at the assumptions accepted may expressed by the equation:

$$V = \frac{\pi}{12} D_{MAX}^2 (3H - D_{MAX}) \tag{10}$$

In deposits with consistent leaching properties, storage caverns are typically leached in a manner that approximates axial symmetry, resulting in a diameter that is roughly two-thirds of the cavern height. For example, if a cavern has a height of 150 m, the maximum diameter (D_{MAX}) could be around 100 m. However, in practical applications, smaller diameters are often chosen to increase the likelihood of achieving regular shapes through the leaching process [34]. In this analysis, a D_{MAX} diameter of 85 m has been assumed. It is worth noting that the minimum thickness of the rock salt layer considered in evaluating the potential for underground hydrogen storage is 150 m, while the maximum thickness is approximately 350 m [26,35]. As a result, the attainable cavern heights within this layer can vary, ranging from 80 m to 280 m. In the present research, it is assumed that the thickness of the salt cavern is approximately 230 m, derived as a linear average of the mentioned thickness range.

The acceptable range of storage pressure for hydrogen storage is contingent upon the depth at which the cavern is located. The maximum pressure is determined based on the depth the cavern neck and is proportional to this depth, with a factor defined as a safe fracturing gradient. To calculate the maximum pressure, the following relationship has been adopted:

$$P_{MAX} = g_f h_N \tag{11}$$

Where, g_f is fracturing gradient, and$h_N$is the depth to the top of the cavern neck.

For hydrogen storage, a safe fracturing gradient value of 0.016 MPa/m has been accepted based on tightness tests [36,37]. This value takes into consideration the higher mobility and permeability of hydrogen compared to natural gas. Adopting this value of the gradient results in a reduction of approximately 11 % in cavern capacity compared to caverns designed for natural gas storage, which have a coefficient of 0.018 MPa/m [38,39]. To justify this assumption, recent case studies and laboratory-scale investigations have confirmed the long-term structural stability of salt caverns under hydrogen-specific conditions. For example, Liu et al. [40] experimentally evaluated the integrity of salt caverns in Germany and showed that caverns remain tight and structurally sound under cyclic hydrogen injection and withdrawal conditions [41]. Similar geomechanical modelling and monitoring efforts in China—particularly in Huai'an and the Jintan salt fields—demonstrated that well-designed salt caverns can safely accommodate hydrogen storage at scale, provided that proper design parameters are maintained [38,42,43]. These findings collectively reinforce the suitability of the adopted fracturing gradient and support the overall feasibility of salt caverns for hydrogen storage.

The minimum pressure required for hydrogen storage depends not only on the depth of the cavern location but also on factors such as the strength of the salt, its creep rate, and the size and shape of the cavern.

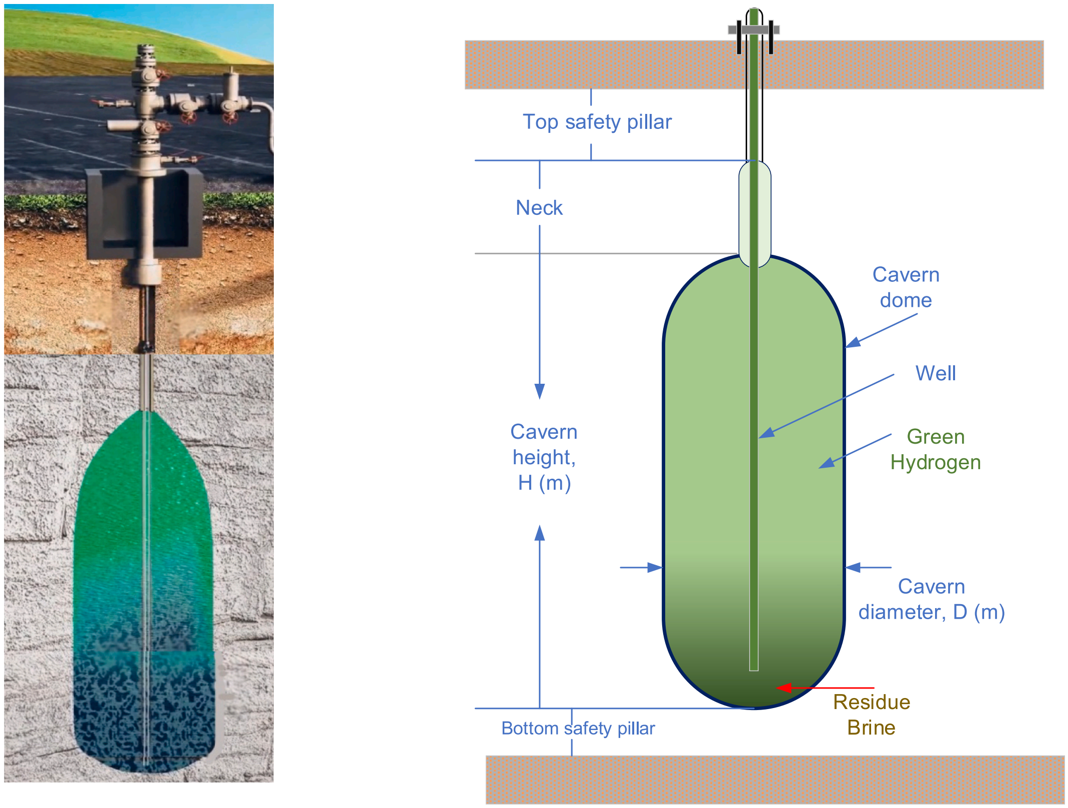

Fig. 4. Illustration of salt cavern simplified shape of the studied cavern [10].

These specific conditions can be approximated using a linear formula.

$$P_{MIN} = g_{\min,p}(h_c - h_0) \tag{12}$$

The gradient of the minimum storage pressure, denoted as $g_{\min,p}$, is determined based on the strength of the rock salt and the distribution of stress within the salt cavern. Meanwhile, h_c represents the depth of the cavern centre, and h_0 refers to the depth of the centre of a cavern that can be completely emptied to a pressure of zero.

The specific minimum and maximum pressure values are directly influenced by the depth of the cavern and the assumed fracturing gradient and minimum storage pressure gradient. These values vary for each individual cavern. Regarding the minimum storage pressure, it is assumed to be the same as that for natural gas and is considered a linear function of the depth of the cavern centre. The amount of gas in the storage cavern at pressure, p, expressed in kilograms is calculated using the following formula;

$$m = f\frac{pV}{ZRT} \tag{13}$$

In the context of gas storage in the cavern, various parameters come into play. These include m, which represents the amount of gas stored in the cavern in kilograms (kg). Additionally, f denotes the proportion of the gross geometric volume filled with gas. The temperature of the stored gas is denoted by T(K), while R represents the gas constant (J/kg K). Finally, the compressibility factor Z is estimated using the Redlich & Kwong Eq. [44], allowing for a better understanding of the behaviour and characteristics of the stored gas within the cavern.

The amount of hydrogen gas in the salt cavern in normal cubic meters can be found as:

$$V_{Nm^3} = \frac{m}{\rho_N} \tag{14}$$

Where ρ_N is the density of the hydrogen in the normal conditions [45].

In addition, knowing cavern volume and temperature, the quantity of cushion gas (CG) required to maintain a minimum.

cavern pressure of 90 bar can be found. The CG densities at 90 bar and cavern temperature of 327.8 K are determined from NIST standard database. Mass of CG is found as:

$$m_{CG} = \rho_{c,min} {}^{*} V \tag{15}$$

Where, V is the cavern volume, and $\rho_{c,min}$ is the density of CG at a minimum cavern pressure of 90 bar and a temperature of 327.8 K.

3.2. *Techno-economic analysis*

Numerous technoeconomic models have been developed to analyse the production costs of hydrogen, revealing that a wide range of hydrogen prices can be achieved. These variations depend on several factors that influence the overall cost structure. Some key factors include government subsidies or incentives, the level of maturity of electrolysis technology, the effective integration of wind power sources, grid infrastructure capabilities, and the efficiency of the electrolyser system.

Government subsidies and incentives play a significant role in reducing the production costs of hydrogen. By providing financial support or favourable policies, governments can encourage investment and promote the growth of the hydrogen industry. Such interventions can help offset the initial capital costs and make hydrogen production economically viable, leading to lower hydrogen prices.

The maturity level of electrolysis technology also impacts hydrogen production costs. As the technology advances and becomes more established, it can benefit from economies of scale, improved efficiency, and reduced manufacturing costs. These advancements result in a decrease in the cost of hydrogen production.

The effective connection of wind power to the electrolyser system and the grid infrastructure is another crucial factor. Wind power, as a renewable energy source, can contribute to lower hydrogen production costs when integrated efficiently. A well-designed system that optimises the connection between wind power generation and electrolysis can lead to cost savings and more competitive hydrogen prices.

Furthermore, the efficiency and reliability of the electrolyser system itself are vital determinants of hydrogen production costs. Technological advancements and improvements in electrolyser designs can enhance efficiency, reduce energy consumption, and lower operational and maintenance costs, all of which contribute to cost optimisation.

In this research, our focus will be on a detailed technoeconomic analysis of salt caverns for hydrogen storage [46], taking into account key variables such as cycling effects. We aim to consider the integrated system, including the hydrogen production part and salt cavern, to understand in what form the Power-X system will be economically viable. However, it is important to highlight that we will not consider the X-power section (gas turbine part) in this research. This aspect will be reserved for future works. By focusing on these elements, we seek to provide a thorough evaluation of the economic and technical feasibility of using salt caverns for hydrogen storage, contributing to the broader understanding and development of efficient hydrogen storage systems. To enhance clarity and transparency for readers, Table 2 presents the key assumptions used in the techno-economic analysis conducted in this study.

To do a comprehensive technoeconomic for the studied salt cavern hydrogen storage, an in-depth and detailed CAPEX and OPEX analysis was conducted. Total direct capital cost (*TDCC*) includes the geologic formation site cost (*GFC*), compressor purchased cost (*CPC*), cushion gas cost (*CGS*), well implementing cost (*WIC*), electrical equipment cost (*EEC*), monitoring device capital cost (MDCC), and surface piping capital cost (*SPCC*) as well as PEM electrolyser capital cost (PEMCC) [47].

$$TDCC(€) = GFC + CPC + CGS + WIC + EEC + MDCC + SPCC + PEMCC \tag{16}$$

The geologic formation site cost (*GFC*) includes the cost of mining (MC) as the following eq. (17) as well as the costs associated with leaching plant (LC), site characterisation cost, and reinforcement cost [48].

$$MC\,(€) = VV\left(m^3\right) \times c_{MC}\left(€/_{m^3}\right) \tag{17}$$

$$LC(€) = m_{H2}(kg) \times c_{LC}\left(\frac{€}{kg_{H2}}\right) \tag{18}$$

Table 2
Assumptions used for the technoeconomic analysis.

Parameter / Term	Assumed Value	Source / Reference
PEM Electrolyser CAPEX	€1600/kW	[49]
Cushion Gas amount	30 % of total H_2 stored	[13]
Cushion Gas cost	~4 [€/kg]	[50]
Mining Cost, c_{MC}	27.57 [€/m^3]	[51,52]
Well Implenetaion Cost, c_{well}	1,378,620 [€/km/well]	[51,52]
leaching plant cost, c_{LC}	5.99 [€/kg H_2]	[51,52]
Electricity Cost	€0.05/kWh	[53]
Water Cooling Cost	€0.0135/kWh	[54,55]
Compressor Power Requirement	1.2 MW per unit	[56]
Compressor Mass Flow Rate	3000 kg/h per unit	[56]
Electrolyser Stack Replacement Frequency	Every 6 years	[57,58]
Discount Rate (Energy-Related OPEX)	12 %	[59]
Discount Rate (Non-Energy OPEX)	5 %	[60]
Plant Lifetime	40 years	[61]
Degradation Rate	2 % per year	[61]
Monitoring Equipment Cost	€5 million (NMR) + €55,000 per cavern (Camera System)	[62]
Hydrogen Pipeline Fixed Cost	€500,000/km	[63]

where VV is the void volume of a cavern in m^3.

The compressor plays a vital role in effectively and safely storing hydrogen in a salt cavern. Its primary function is to pressurise the hydrogen to the desired level and ensure a smooth injection into the cavern. Moreover, the compressor should operate reliably, continuously, and respond promptly to meet the demand for hydro gen when required. The compressor purchased cost (*CPC*) can be calculated as follows [64];

$$CPC\,(€) = CUC\left(€/_{kW}\right) \times N_{comp} \times \dot{W}_{comp} \tag{19}$$

Where *CUC* is the compressor unit cost, N_{comp} is the number of compressor and $\dot{W}_{comp}$ represents size of the compressor.

The cost of cushion gas is a significant factor that impacts the overall cost of the storage system. It is assumed that the cost of cushion gas is directly linked to the price of purchased hydrogen from the hydrogen production side. Cushion gas refers to the quantity of gas necessary to be present in the cavern to maintain a stable pressure for the working gas. Different gases, such as hydrogen itself, nitrogen, carbon dioxide, and methane, can be used as cushion gas options.

Based on available literature, it is commonly considered that approximately 30 % of the total hydrogen gas stored in the cavern is allocated as cushion gas. To calculate the cushion gas cost (*CGS*), the following formula can be used:

$$CGS\,(€) = c_{H_2} \times m_{CG} \tag{20}$$

Where m_{CG} is the total cushion gas required for each cavern and c_{H_2} is the hydrogen purchased cost (€/*kg*) that is going to be stored in the salt cavern.

In the present study, the implementation cost associated with drilling and constructing a well for creating a structurally sound salt cavern and injecting hydrogen is taken into account. This cost is referred to as the well implementation cost (*WIC*). The expenses incurred for drilling and establishing the well structure are important considerations in the overall economic analysis of the hydrogen storage system.

$$WIC(€) = c_{well} \times L_{well} \times N_{well} \tag{21}$$

The electrical equipment cost (*EEC*) includes the costs associated with transformer capital cost, electricity circuit breaker price, transformer erection and installation cost, instrumentation and controls.

Monitoring hydrogen storage in underground salt caverns is very challenging and fraught with uncertainty regarding the precise equipment required. Although technologies such as MMV (Measurement, Monitoring, and Verification) and NMR (Nuclear Magnetic Resonance) exist, we have chosen to consider NMR. In our techno-economic analysis of hydrogen storage in salt caverns, we included the Monitoring Device Capital Cost (MDCC). This encompasses a €5 million investment for NMR sensors and an additional €55,000 per cavern for the CUES C550 Crawler Camera System, both used for subsurface imaging. This comprehensive inclusion ensures a detailed and accurate assessment of the costs involved, enhancing the reliability of our economic evaluation.

To facilitate the transfer of hydrogen from the supply point to the storage facility, it is necessary to employ surface hydrogen piping infrastructure cost (SPIC) including surface pipeline capital cost (SPCC) and temporary hydrogen storage tanks (THST). These components play a crucial role in ensuring a smooth and efficient transportation process. The surface hydrogen piping serves as the conduit for conveying the hydrogen from its source to the storage point, while the temporary storage tanks provide a means to hold the hydrogen temporarily before it is injected into the designated storage facility.

$$SPIC\,(€) = SPCC_{H_2} + THST_{H_2} \tag{22}$$

$$SPCC_{H_2} = c_{H_2,sp} \times L_{H_2,p} \tag{23}$$

$$THST_{H_2} = c_{H_2,ST} \times V_{ST} \tag{24}$$

Where $c_{H_2,sp}$ and $c_{H_2,ST}$are hydrogen pipeline fixed cost per km and hydrogen storage capital cost, respectively. In addition, $L_{H_2,p}$ denotes the pipeline length and $V_{ST}$is the size of the temporary storage tank.

The most recent information regarding the price of PEM electrolysers, based on their power in euros per kW at the scale of MW, indicates that the cost generally ranges from €1200 to €2000 per kW. This translates to approximately €1.2 million to €2 million per MW for large-scale applications, as reported by the Oxford Institute for Energy Studies. For our analysis, we have assumed an average cost of €1600 per kW for the PEM electrolyser [49].

To provide more realistic on the costs, indirect costs including 10 % of Total direct capital cost (*TDCC*) as an engineering and supervision (ES) cost, 10 % as a construction cost including temporary facilities, and insurance (CC) and 10 % as contingencies are added to yield the fixed capital investment cost as follows;

$$FCI\,(€) = TDCC\,(€) + ES(€) + CC(€) + \text{Contingencies}(€) \tag{25}$$

The total capital investment can be determined by incorporating additional expenditures into the fixed capital investment cost. These additional costs include licensing, research, and development (LRD) expenses, as well as the Allowance for Funds Used During Construction (AFUDC), which accounts for the funds employed during the construction phase. To calculate the total investment cost, these outlays are added to the fixed capital investment cost, typically at a rate of 10 %. The calculation for the total investment cost is as follows:

$$TCI\,(€) = FCI(€) + OO(€) \tag{26}$$

The operating and maintenance cost of the system comprises both the total fixed O&M cost (TFOM) and the variable O&M cost (VOM). The calculation of the TFOM involves considering 5 % of the total cost of the purchased equipment.

On the other hand, the calculation of the variable costs incorporates the electrical power required by the compressor and the associated costs of compressor cooling. These factors contribute to the determination of the TVOM, which accounts for the varying expenses incurred during the operation and maintenance of the system.

$$OPEX\,(€/yr) = TFOM(€/yr) + TVOM(€/yr) \tag{27}$$

The calculation of the Total Variable O&M cost (TVOM) involves specific considerations. In this analysis, the electricity cost for the compressor is assumed to be €0.05 per kilowatt-hour (kWh), and the cost for using water cooling to provide the necessary compressor cooling is estimated at €0.0135 per kWh. We have selected a compressor with a capacity to compress hydrogen at a mass flow rate of up to 3000 kg/h per unit, with a maximum power requirement of 1.2 MW. This system will be scaled up to meet the proposed scenario targets in terms of power and injection mass flow rate. For the electrolyser, we have assumed a stack replacement every six years throughout the plant's lifetime, with a reasonable 50 % capacity factor for the electrolyser.

Finally, the Levelised Cost of Hydrogen (LCOH) storage for the proposed salt cavern can be calculated as the following equation;

$$LCOH = \frac{c_{inv} + \sum_{y=1}^{N} \frac{c_{opex,y}}{(1+d)^y}}{\frac{\sum_{y=1}^{N} H_{2,y} \times (1-R_{deg})^y}{(1+R_{deg})^y}} \tag{28}$$

Where c_{inv} is the total investment cost, $c_{opex,y}$ is the operating and maintenance cost for the Nth year, d is the discount rate which is assumed to be 12 % for energy related OPEX and 5 % for other non-energy related OPEX contributors, and N is the plant lifetime assumed to be 40 years for hydrogen storage operation, R_{deg} is the degradation rate which is assumed to be 2 %. In addition, $H_{2,y}$ is the total stored hydrogen for the Nth year.

4. Results and discussion

4.1. Technical results

Based on the method used in this study, the void volume of each cavern is estimated to be 480,000 cubic meters. Considering the 90 bar pressure required for the cushion gas, the amount of cushion gas, on a mass basis, is approximately 3.5 million kilograms, which equals nearly 37 million standard cubic meters (Sm^3) of hydrogen. Results revealed that by considering the constraint of a 10 bar injection limitation per day to maintain cavern integrity, we can expect the total mass of working gas hydrogen to be around 7.5 million kilograms, equivalent to nearly 90 million Sm^3. In this context, the ratio of cushion gas to working gas will be approximately 30 % to 70 %.

It should be noted that this amount of gas and energy is for one cavern, without any cycling or continuous withdrawal rate. The energy stored in the working gas can be calculated as 255 GWh. This calculation provides a comprehensive overview of the hydrogen storage capabilities and emphasizes the significant energy storage potential within a single cavern, considering both cushion and working gas requirements.

Fig. 5 illustrates the amount of working gas storable and the energy storage potential as the number of salt caverns increases, both with and without the cycling effect. The bar chart shows a clear trend where the amount of working gas storable (in kg of H_2) and the corresponding energy stored (in TWh) both increase as the number of caverns increases. Without the cycling effect, the storage capacity is significantly lower, demonstrating the importance of cycling in enhancing the storage potential. For instance, with seven caverns, the amount of working gas stored is notably higher with cycling, reaching around 300,000 t of H_2 and an energy storage potential of about 10 TWh, compared to much lower values without cycling. This highlights the effectiveness of cycling in maximising the storage capabilities of salt caverns.

Fig. 6 illustrates the relationship between the number of days required to fill a cavern and the number of compressors installed in parallel. The graph shows a clear decreasing trend in the number of days required as more compressors are added. Starting with one compressor, it takes 247 days to fill a cavern. However, with eight compressors operating in parallel, the time required reduces significantly to approximately 31 days. The trend suggests a non-linear relationship where each additional compressor leads to progressively smaller reductions in the number of days required. The dashed line represents the maximum power output in MW, indicating a proportional increase with the number of compressors and highlighting the efficiency gains from parallel compressor operations in reducing filling time. It is important to note that a compressor with a power of 1.2 MW and a maximum flow rate of 3000 kg hydrogen per hour is selected as the base compressor unit.

Although increasing the compressor power will definitely reduce the number of days required to fill a cavern, it poses a significant challenge in terms of providing such a high flow rate of hydrogen. This challenge will be discussed in terms of the PEM electrolyser capacity and size. Scaling up the hydrogen production to match the increased compressor power demands significant enhancements in the PEM electrolyser system, including larger capacity units and more advanced technology to ensure consistent and efficient hydrogen production. Addressing these challenges is crucial for the practical implementation of high-capacity hydrogen storage systems.

Fig. 7 illustrates the relationship between electricity generation from a wind farm and the resulting hydrogen production rate over a year. The blue line represents the electricity generation from the wind farm with a maximum capacity of 21 MW, while the green line indicates the hydrogen production rate in kg/h.

From the available data for the selected wind farm, it has been calculated that hydrogen can be produced at an average rate of 164.8 kg/h. This corresponds to a capacity factor of approximately 44 % for the electrolyser, indicating how effectively the electrolyser is utilised

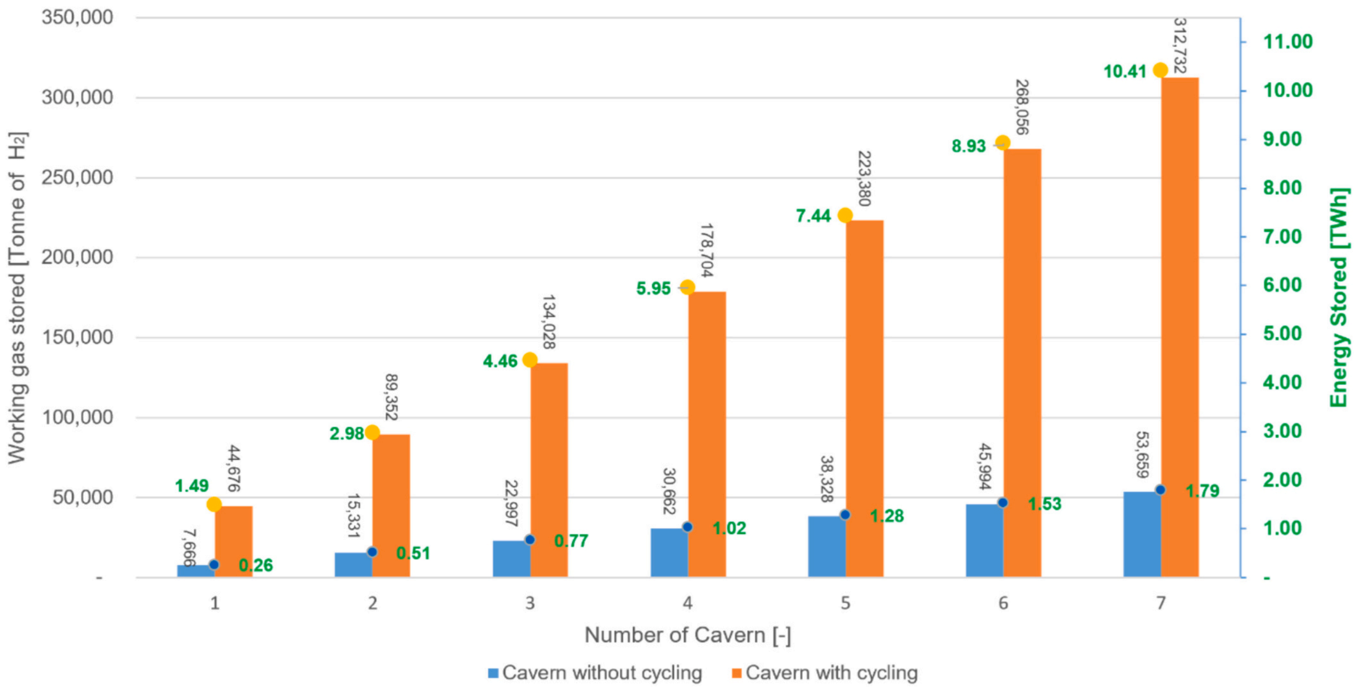

Fig. 5. Amount of working gas storable and energy storage potential by an increase in the number of salt caverns with/without cycling effect.

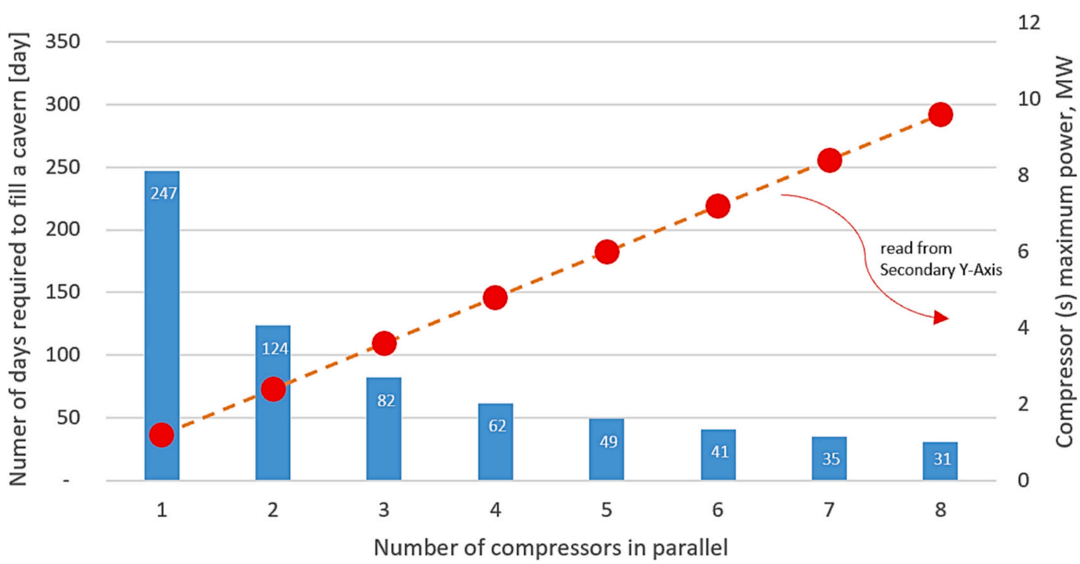

Fig. 6. Number of days required to fill a cavern versus the number of compressors installed in parallel.

relative to its maximum potential output.

To ensure continuous operation of the PEM electrolyser, it is assumed that a minimum of 1.5 MW power needs to be supplied at all times. When wind power is insufficient or unavailable, this power requirement must be met by drawing electricity from the grid. This ensures that hydrogen production can continue uninterrupted, maintaining the efficiency and reliability of the storage system.

Importantly, based on this average hydrogen production rate, it would take almost 6 years to fill a storage cavern. This calculation assumes continuous operation without any interruptions or downtime. The graph clearly demonstrates the variability in both electricity generation and hydrogen production, which is typical of wind power due to fluctuating wind speeds throughout the year. This variability must be considered when planning for hydrogen storage and its subsequent use in energy applications.

4.2. Technoeconomic results

In our study, we first focused on examining the CAPEX and OPEX for a single salt cavern used for hydrogen storage, incorporating the purchased cost of PEM electrolysers. This initial analysis provided a detailed assessment of the economic feasibility of hydrogen storage in one cavern. Additionally, we evaluated the impact of increasing the number of caverns on the overall storage potential and cost-effectiveness. By scaling up the number of caverns, we aimed to enhance the hydrogen storage capacity and analyse the corresponding changes in total CAPEX and OPEX. Our comprehensive technoeconomic analysis covers key aspects such as the costs associated with cushion gas, compressor systems, and the operational efficiency of PEM electrolysers, offering valuable insights into the practical implementation of large-scale hydrogen storage solutions.

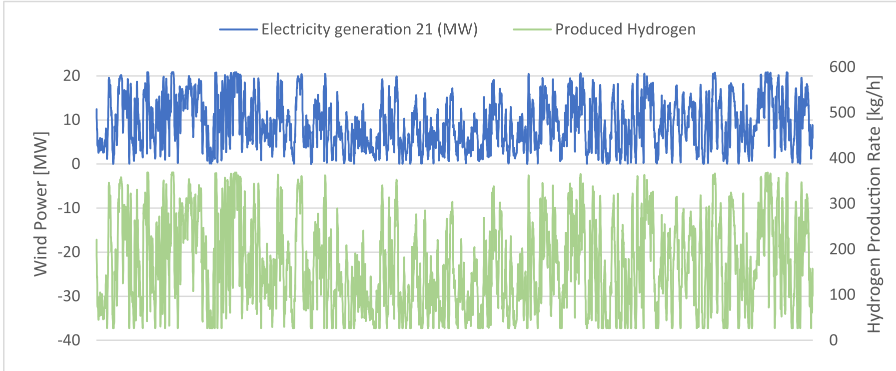

Fig. 7. Wind power and hydrogen production rate for the studied year.

Fig. 8 details the total investment cost breakdown for implementing a new hydrogen storage cavern, which amounts to nearly €270 million, excluding the PEM electrolyser cost. The largest contributor to this cost is the Geologic Formation Site Cost (GFC), which stands at about €115.5million, highlighting the substantial costs involved in preparing the geological site for the cavern. Following this, the Compressor Purchased Cost (CPC) is the second-largest expense, totalling in excess of €25 million.

The Cushion Gas Cost (CGS) contributes just over €9 million, while the Well Implementing Cost (WIC) adds about €3 million, covering the expenses associated with drilling and constructing the well structure. The Electrical Equipment Cost (EEC) amounts to €3.4 million, which includes transformers, circuit breakers, and other essential electrical equipment. Monitoring Device Capital Cost (MDCC) allocated €6 million for Nuclear Magnetic Resonance (NMR) sensors and CUES C550 Crawler Camera Systems for subsurface imaging. The Surface Piping Capital Cost (SPCC) totals €3.8 million for the necessary hydrogen piping infrastructure.

In addition to these direct costs, there are significant indirect costs: Engineering and Supervision (ES) and Construction Costs Including Temporary Facilities and Insurance (Construction), each estimated at €15.8 million. Contingencies, which account for unexpected expenses, amount to €20 million. Lastly, the Costs of Licensing, Research, and Development (LRD), and the Allowance for Funds Used During Construction (AFUDC) collectively total €25 million. This comprehensive breakdown highlights the major cost contributors, emphasising the significant financial requirements for the successful establishment of a hydrogen storage cavern.

The breakdown of the CAPEX for building a single hydrogen cavern, as illustrated in Fig. 9, highlights the major cost contributors associated with the total direct cost, excluding indirect costs and other outlays. The largest contributor is the Geologic Formation Site Cost (GFC), which accounts for 67.7 % of the total direct CAPEX. This significant percentage is due to the extensive geological work required to prepare and

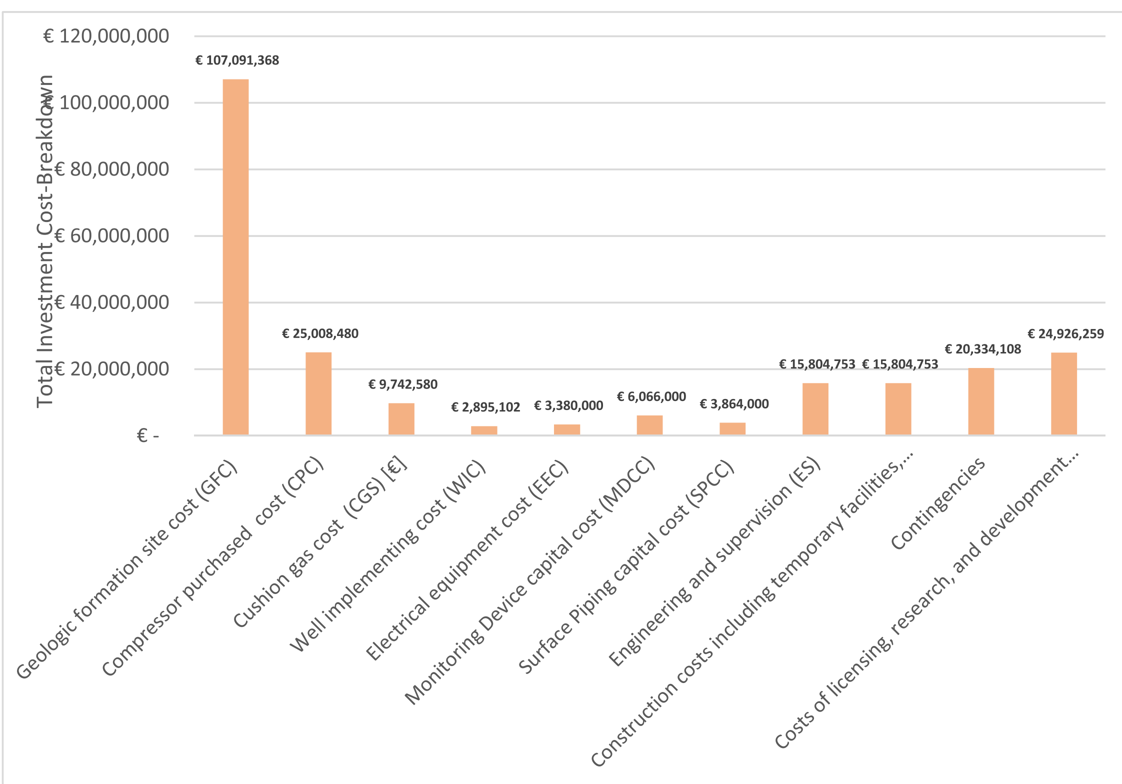

Fig. 8. Total investment breakdown for implementing a single cavern for hydrogen storage.

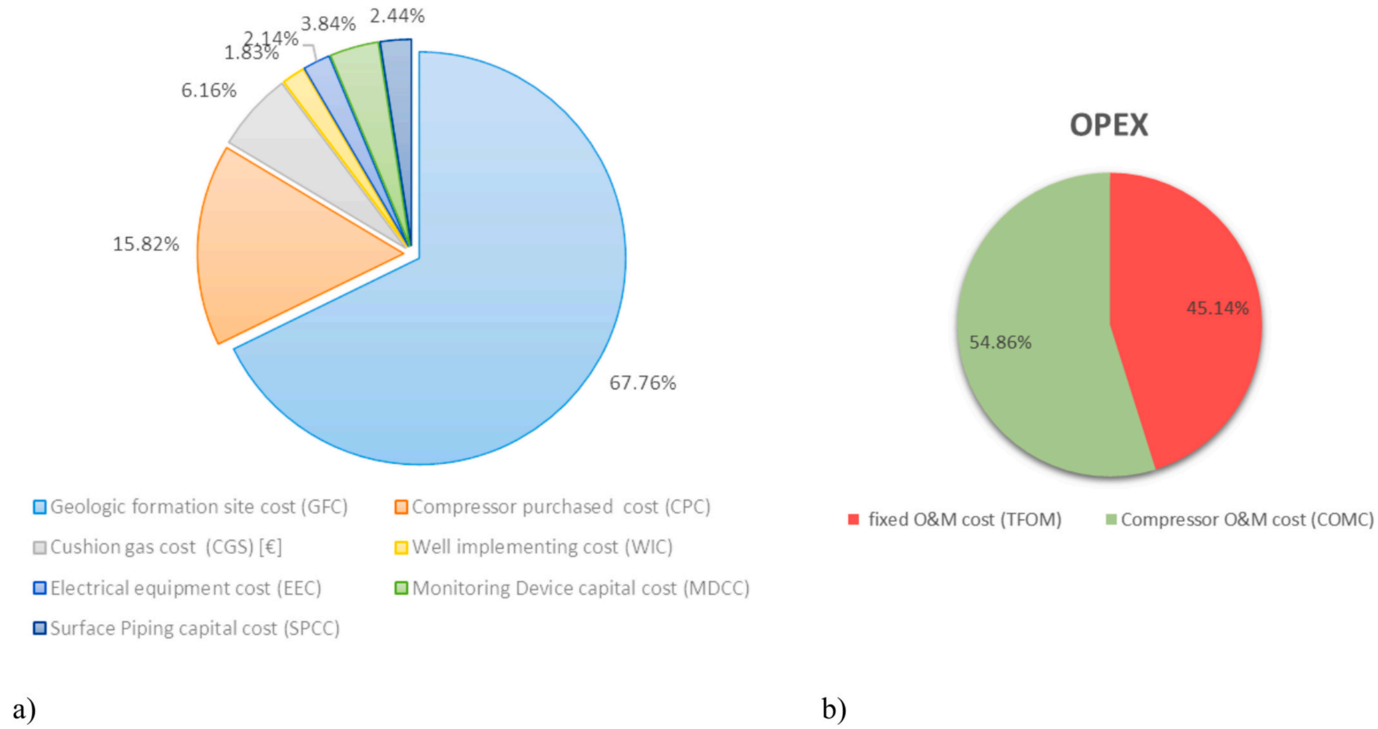

Fig. 9. a) CAPEX and b) OPEX breakdowns for building single hydrogen cavern.

maintain the underground storage site, emphasising the need for focused investment in this area. The Compressor Purchased Cost (CPC) is the second-largest contributor, making up 15.8 % of the total direct CAPEX. This reflects the necessity for robust compressors capable of handling large volumes and high pressures, highlighting the critical role of reliable compression technology. The Cushion Gas Cost (CGS) follows, representing 6.2 %. This cost is essential for maintaining the minimum pressure in the cavern, underscoring its importance in the overall storage system. Monitoring Device Capital Cost (MDCC) accounts for 3.8 %, covering advanced imaging and monitoring technologies, which are crucial for ensuring the safety and integrity of the storage facility. Surface Piping Capital Cost (SPCC) is 2.4 %, allocated for the surface infrastructure, and Electrical Equipment Cost (EEC) represents 2.1 %, including transformers and circuit breakers necessary for the operation. The Well Implementing Cost (WIC) is the smallest contributor, at 1.8 %, covering expenses related to drilling and constructing the wells. The total direct cost for building a single hydrogen cavern is nearly 160 million euros, driven by the technical and safety requirements essential for creating a viable and secure hydrogen storage solution. This breakdown highlights the areas requiring more focus and investment, particularly the geological formation and compression systems, which constitute the largest portions of the CAPEX.

The operational expenditure (OPEX) for this system is estimated to be around €4.6 million annually. Of this, approximately 45 % is allocated to fixed O&M costs (TFOM), which include routine maintenance and operational activities. The remaining 55 % is dedicated to the compressor O&M cost (COMC), reflecting the significant role of compressors in the overall operational costs. This includes the electricity consumption and cooling requirements for the compressors, underscoring their substantial impact on the annual OPEX. The high proportion of OPEX attributed to compressors highlights the importance of optimising their efficiency and operational reliability to manage costs effectively.

To complement the compressor performance analysis presented in Fig. 6, a cost breakdown sensitivity analysis was performed and is now illustrated in Fig. 10. This figure presents the CAPEX and OPEX with increasing numbers of compressors, providing deeper insight into the economic implications of compressor sizing.

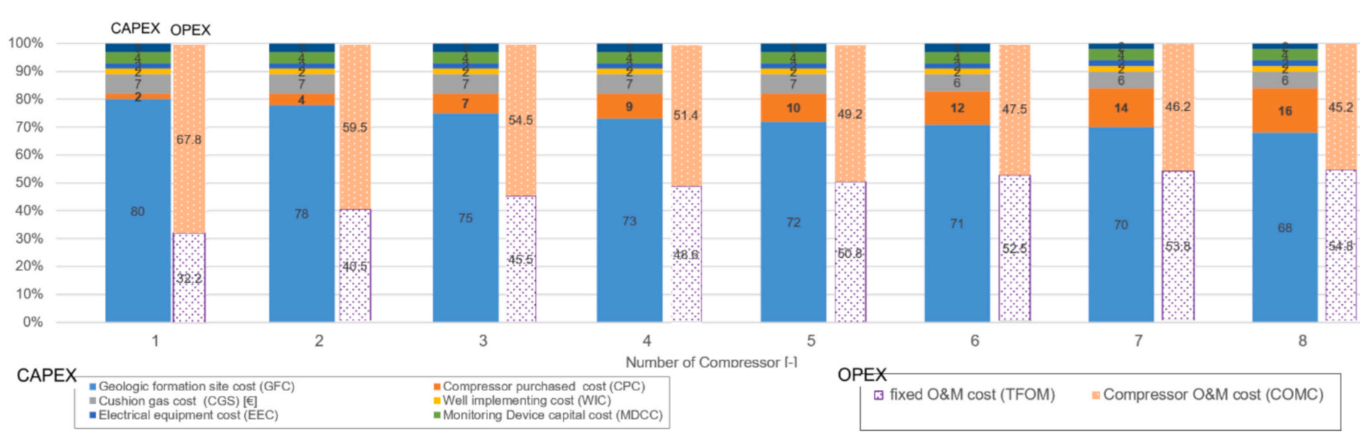

Fig. 10. Effect of compressor number on CAPEX and OPEX cost breakdown.

From the CAPEX perspective, GFC dominates the overall investment across all configurations, though its relative share decreases from 80 % to 68 % as the number of compressors increases from 1 to 8. This shift is offset primarily by a steady rise in CPC, growing from 2 % to 16 %. The trend reflects the direct capital burden associated with adding more compression capacity. In parallel, the OPEX profile reveals an inverse pattern. The COMC declines proportionally (from 67.8 % to 45.2 %) due to cost distribution across more units, while the TFOM grows in relative significance (from 32.2 % to 54.8 %). This transition underscores how increasing system complexity drives up base-level support and infrastructure maintenance requirements, even as individual compressor costs decline.

Together, these results highlight a key trade-off: although adding more compressors can reduce operational time, it also introduces non-linear increases in both CAPEX and fixed OPEX. The economic gains from further compression beyond a certain point diminish, suggesting that a configuration with 5–6 compressors may offer the most cost-effective balance between speed and investment. These insights are particularly valuable for planning large-scale hydrogen storage systems under budgetary and infrastructure constraints.

Fig. 11 demonstrates the effect of increasing the number of caverns on the levelised cost of hydrogen storage. The trend indicates a decrease in the levelised cost as the number of caverns increases. Starting at €0.52/kg for a single cavern, the cost drops to €0.43/kg with two caverns, and further to €0.42/kg with three caverns. This downward trend continues, reaching €0.38/kg when seven caverns are utilised. The reduction in levelised cost can be attributed to economies of scale, where the fixed costs are distributed over a larger storage capacity, thereby lowering the cost per kilogram of stored hydrogen. Additionally, operational efficiencies and improved utilisation of infrastructure contribute to the reduced costs with an increased number of caverns. This trend highlights the economic advantage of expanding the storage capacity to achieve a more cost-effective hydrogen storage solution.

Fig. 11 also illustrates the impact of increasing the number of salt caverns on the LCOH storage, both with and without cycling effects. The LCOH decreases as the number of caverns increases, highlighting the economies of scale in hydrogen storage. When cycling is considered, the LCOH starts at €0.52/kg H_2 with one cavern and decreases to €0.38/kg H_2 with seven caverns. Without cycling, the LCOH begins at a significantly higher value of €2.37/kg H_2 and decreases to €1.91/kg H_2 for seven caverns.

The cycling effect drastically reduces the LCOH, showing its importance in optimising storage costs. However, implementing cycling requires a substantial amount of hydrogen, significantly impacting the size and capacity of the required PEM electrolyser. This creates pressure on hydrogen production facilities to meet the high hydrogen demand.

To address this, alternative strategies such as integrating a hydrogen gas network or deploying multiple smaller electrolysers across the country might be more viable solutions. These methods could efficiently distribute the hydrogen production load, ensuring a stable and scalable supply to meet the storage demands.

Fig. 12 presents very interesting results regarding the impact of PEM electrolyser size on the levelised cost of hydrogen (LCOH) and the time required to fill a cavern with produced hydrogen. It can be stated when employing a large cavern capable of storing almost 7.5 million kg of hydrogen per cycling, using a small PEM electrolyser proves to be inefficient both in terms of time and cost. Specifically, a 20 MW PEM electrolyser, operating at full load, requires nearly 2.5 years to fill the cavern and results in a high LCOH of approximately €10 per kg. This inefficiency underscores the economic unviability of such a setup, emphasising the need for larger electrolyser capacities or alternative strategies.

The results demonstrate that increasing the capacity of the PEM electrolyser, although it significantly raises the total CAPEX and OPEX, effectively reduces the LCOH and the filling duration. For instance, utilising a 200 MW PEM electrolyser reduces the filling time to about 90 days, making it feasible to achieve three cycling periods within a year. This reduction in time and cost is critical for making the hydrogen storage project economically viable.

However, the challenge of supplying such a large volume of hydrogen remains. This necessitates governmental support to address the chicken-and-egg problem of hydrogen infrastructure development. Without an assured hydrogen flow rate, investing in large-scale electrolysers and storage caverns the prospect is risky for developers and investors. One potential solution is to distribute electrolysers across different hydrogen production hubs nationwide, creating an active hydrogen pipe network to facilitate the transfer and pressurisation of hydrogen into caverns as needed. In addition, practical barriers such as grid connection constraints, permitting timelines, and supply chain bottlenecks must be addressed to enable the deployment of large-scale electrolysers (e.g., 200 MW and above). High-capacity systems require robust and flexible grid infrastructure to manage variable loads and ensure stable operation. At the same time, permitting processes for large electrolysis plants can be lengthy and uncertain, often involving

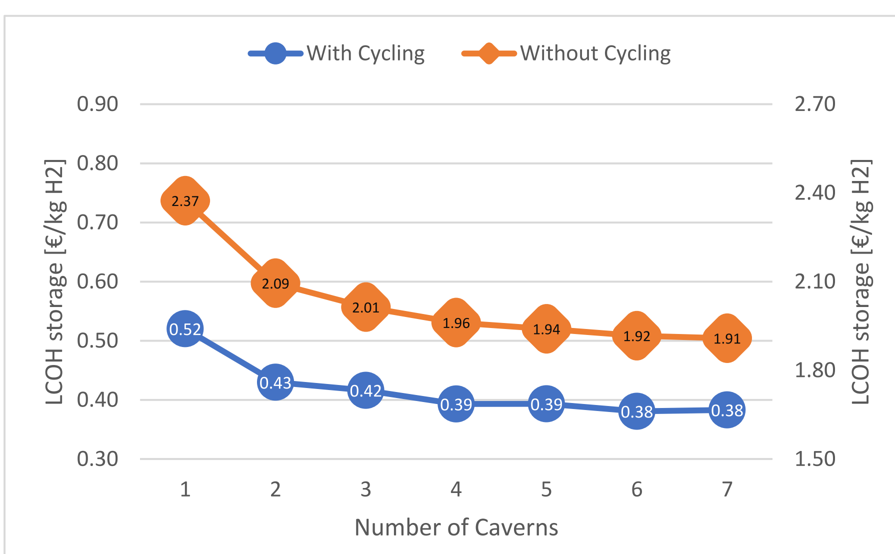

Fig. 11. Effect of increasing the number of caverns on levelised cost of hydrogen storage.

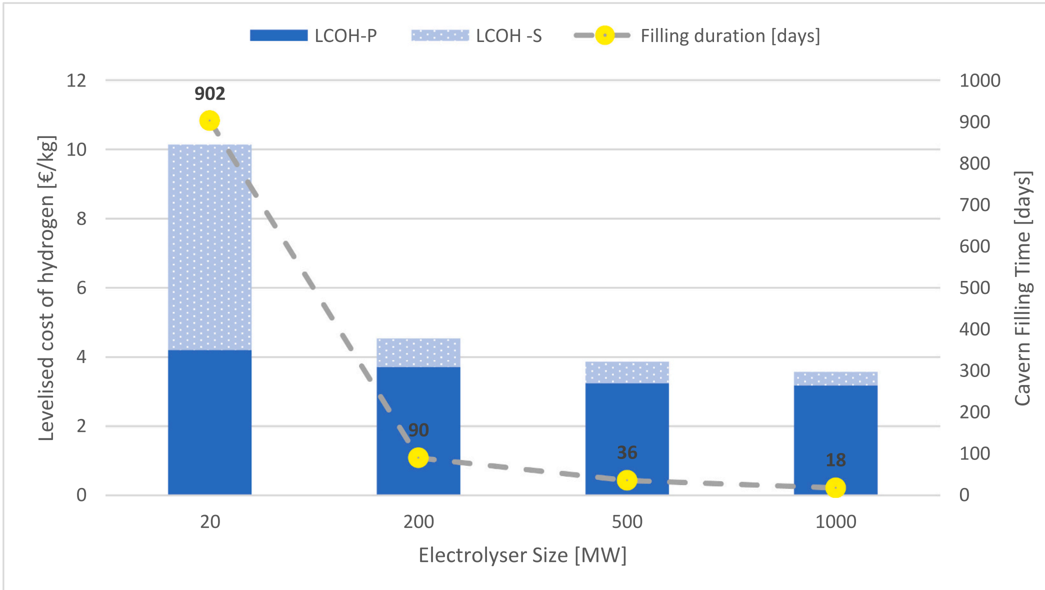

Fig. 12. Effect of PEM electrolyser size on the levelised cost of hydrogen (P - production & S - storage) as well as on the filling a cavern with produced hydrogen.

complex environmental and regulatory approvals. Moreover, the availability of key components such as PEM stacks and power electronics at gigawatt scales remains limited. To overcome these obstacles, strategic policy support is essential—through mechanisms such as accelerated permitting pathways, financial incentives, and grid planning that prioritizes hydrogen hubs. Addressing these practical challenges will be critical to realizing the envisioned hydrogen infrastructure at scale.

To assess the robustness of the system design and its cost drivers, a sensitivity analysis is performed considering ±20 % variations in key parameters for the 200 MW electrolyser Scenario. The impact of these variations on the Levelised Cost of Hydrogen for both storage (LCOH-S) and production (LCOH-P) is presented in Fig. 13.

For LCOH-S, the most influential parameters were identified as the system degradation rate and leaching price. A ± 20 % variation in degradation leads to a significant change in LCOH-S from €0.66/kg to €1.04/kg, while changes in leaching price affect the cost from €0.77/kg to €0.89/kg. These results underscore the importance of durability and site-specific operational costs in underground hydrogen storage.

For LCOH-P, the analysis revealed that PEM electrolyser efficiency and degradation are the most critical factors. Improving PEM efficiency reduces LCOH-P from €5.13/kg to €2.86/kg, demonstrating its strong influence on overall production economics. Similarly, degradation variations cause LCOH-P to shift between €3.09/kg and €4.32/kg.

Overall, these findings highlight the importance of hydrogen storage and the need from government to have strategic planning and investment in hydrogen infrastructure to ensure economic viability and efficient operation of large-scale hydrogen storage systems in a timely manner to enable deployment of renewable energy targets enabling energy security.

5. Summary and conclusion

In our study, we explored the integration of wind power with hydrogen storage in salt caverns, focusing on the technical and economic viability of such systems. Leveraging the wind resources in Ireland, the produced hydrogen is stored in salt caverns, which offers a robust solution to manage the intermittency of renewable energy and ensure a stable energy supply.

The technoeconomic analysis highlighted several key points. The void volume of each cavern is estimated at 480,000 cubic meters, with approximately 3 million kilograms of cushion gas required to maintain a pressure of 90 bar. The working gas capacity was found to be around 7.5 million kilograms, equivalent to nearly 90 million standard cubic meters of hydrogen, with an energy storage potential of 255 GWh.

We assessed the CAPEX and OPEX for a single cavern. The total investment cost for a single cavern, excluding the PEM electrolyser, is approximately €240 million, with the largest contributors being the geologic formation site cost and compressor purchase cost. The direct

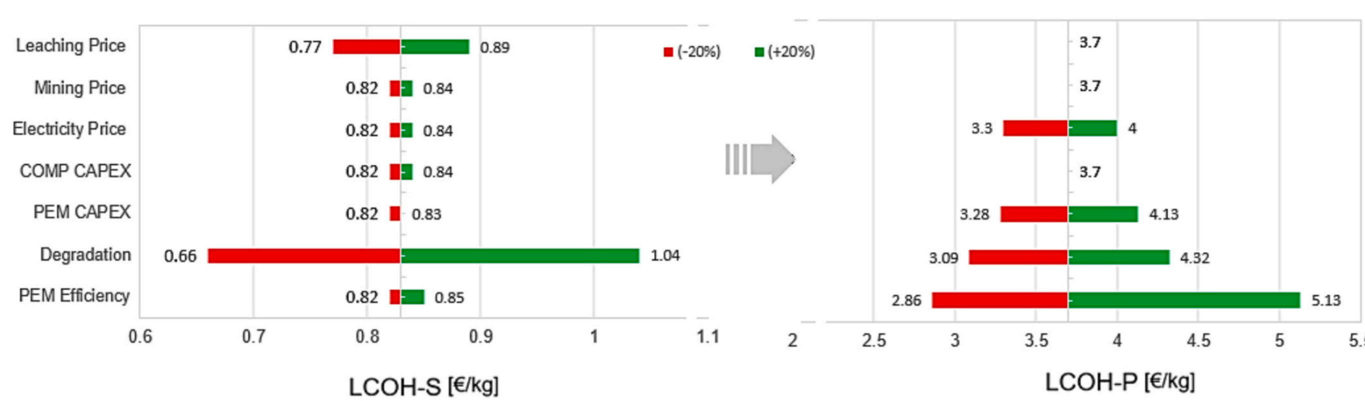

Fig. 13. Sensitivity of LCOH production and storage to ±20 % changes in key parameters.

costs, driven by technical and safety requirements, are substantial. The CAPEX breakdown shows the geologic formation site cost as the most significant, followed by compressor purchase and well implementing costs. The OPEX is estimated at €4.6 million annually, with compressors consuming nearly half of this due to their electricity and cooling demands.

Expanding the number of caverns significantly reduces the LCOH. For instance, increasing from one to seven caverns decreases the LCOH from €0.52/kg to €0.38/kg due to economies of scale. This trend underscores the economic benefits of scaling up storage capacity. Moreover, implementing cycling to enhance storage efficiency requires substantial hydrogen volumes, pressuring the PEM electrolyser capacity.

We also examined the effect of PEM electrolyser size on the LCOH and cavern filling duration. Smaller electrolysers, like the 20 MW unit, are inefficient, taking nearly 2.5 years to fill a cavern and resulting in a high LCOH of €10/kg. In contrast, larger electrolysers, such as the 200 MW unit, significantly reduce both the LCOH and filling duration, demonstrating economic viability with a filling time of 90 days and enabling three cycling periods per year. However, the challenge remains in supplying such large hydrogen volumes, which may require a distributed network of electrolysers and governmental support to ensure a stable hydrogen supply.

Although the technoeconomic analysis proved that using green hydrogen as cushion gas could yield the final levelised cost of hydrogen storage in a reasonable range (€0.38 to €2 per kilogram in the worst scenario), the market today is not ready to produce such large amounts of green hydrogen on-site. One possible solution might be to use blue hydrogen produced through SMR + CCS (Steam Methane Reforming with Carbon Capture and Storage) as the cushion gas during the initial stages. This approach can help the market become operationally ready, addressing the chicken-and-egg problem of hydrogen supply and demand. Also, it is important to consider that leaching a new cavern and filling it with cushion gas technically takes several years, so meticulous decision-making is needed given the substantial investment required. Conducting thorough risk management is highly recommended to mitigate potential challenges.

In conclusion, the integration of wind power with hydrogen storage in salt caverns is a promising solution for large-scale energy storage, offering economic and technical feasibility. Strategic planning and investment in hydrogen infrastructure are crucial for realizing these benefits, addressing the challenges of hydrogen supply, and supporting the transition to a sustainable and low-carbon future.

6. Research limitations and future work

While the techno-economic analysis in this study demonstrates the feasibility and cost-effectiveness of using salt caverns for hydrogen storage, it is essential to acknowledge the associated geological challenges that may influence real-world deployment. These include cavern stability over time, potential gas leakage due to microfractures or imperfect sealing, and the long-term integrity of the salt formation under repeated cycling. The design assumptions used in this work are based on idealised cavern conditions and established safety margins; however, actual performance depends heavily on site-specific geomechanical characteristics, such as rock salt creep, interbedded impurity layers (e.g., clay or anhydrite), and local tectonic activity.

In particular, hydrogen leakage—although minimal in well-characterised caverns—remains a potential concern over long durations. A recent study examining hydrogen storage in the Jintan salt cavern in China reported an estimated leakage rate of approximately 0.36 % over 30 years of cyclic operation, primarily due to viscous flow through microfractures and surrounding formations [65]. Factors such as operating pressure, cavern geometry, and the mineralogical composition of the salt formation influence leakage behaviour. While these leakage rates are relatively low and within acceptable limits, they highlight the importance of rigorous site screening, pressure management, and implementation of long-term monitoring protocols—such as MMV (Measurement, Monitoring, and Verification) systems.

These geological risks and uncertainties merit further investigation in future work, particularly as Ireland and other regions evaluate the suitability of their salt formations for hydrogen storage. Incorporating detailed geotechnical modelling and empirical site data will be crucial to ensuring safe, stable, and scalable deployment of underground hydrogen storage infrastructure.

CRediT authorship contribution statement

Ali Saberi Mehr: Writing – review & editing, Writing – original draft, Visualization, Validation, Supervision, Software, Resources, Project administration, Methodology, Investigation, Formal analysis, Data curation, Conceptualization. **James G. Carton:** Writing – review & editing, Writing – original draft, Supervision, Project administration, Methodology, Funding acquisition, Data curation, Conceptualization.

Declaration of competing interest

The authors declare the following financial interests/personal relationships which may be considered as potential competing interests: James G Carton reports financial support was provided by MaREI the SFI Research Centre for Energy Climate and Marine. If there are other authors, they declare that they have no known competing financial interests or personal relationships that could have appeared to influence the work reported in this paper.

Acknowledgments

The authors gratefully acknowledge the support extended by Dublin City University, MaREI, and the industrial partners participating in the HyLIGHT project (https://www.marei.ie/project/hylight/). This research and collaborative effort have received partial funding from Science Foundation Ireland through MaREI, the SFI Research Centre for Energy, Climate, and Marine [Grant No: 12/RC/2302_P2 (HyLIGHT)], with additional financial backing provided by the project's 26 industry partners.

Data availability

Data will be made available on request.

References

[1] Renewable energy – powering a safer future n.d. https://www.un.org/en/climatechange/raising-ambition/renewable-energy (accessed June 23, 2024).
[2] A. Agarwala, T. Tahsin, M.F. Ali, S.K. Sarker, S.H. Abhi, S.K. Das, et al., Towards next generation power grid transformer for renewables: Technology review, Eng. Rep. 6 (2024), https://doi.org/10.1002/eng2.12848.
[3] J. Rogers, S. Fink, K. Porter, Subcontract Report Examples of Wind Energy Curtailment Practices, 2010.
[4] S. Canbulat, K. Balci, O. Canbulat, I.S. Bayram, Techno-economic analysis of on-site energy storage units to mitigate wind energy curtailment: A case study in Scotland, Energies (Basel) 14 (2021) 1691.
[5] Martínez SM, Lázaro EG, Escribano AH, Carretón MC, Molina-Garcia A. Wind Power Curtailment Analysis under generation flexibility requirements: The Spanish case study. 2015 IEEE power & Energy society general meeting, IEEE; 2015, p. 1–5.
[6] Aziz M. Liquid hydrogen: A review on liquefaction, storage, transportation, and safety. Energies (Basel) 2021;14:5917.
[7] Y. Kojima, M. Yamaguchi, Ammonia as a hydrogen energy carrier, Int. J. Hydrog. Energy 47 (2022) 22832–22839.
[8] M.M. Hasan, M.G. Rasul, M.I. Jahirul, M.A. Sattar, N.M.S. Hassan, Hydrogen horizons: Navigating challenges and opportunities for a sustainable Energy future, in: 2023 International Conference on Sustainable Technology and Engineering (I-COSTE), IEEE, 2023, pp. 1–7.
[9] Y. Son, H. Cha, C. Jo, A.S. Groombridge, T. Lee, A. Boies, et al., Reliable protocols for calculating the specific energy and energy density of Li-ion batteries, Mater Today Energy 21 (2021) 100838.

[10] S. Hui, S. Yin, X. Pang, Z. Chen, K. Shi, Potential of salt caverns for hydrogen storage in southern Ontario, Canada, Mining 3 (2023) 399–408, https://doi.org/10.3390/mining3030024.
[11] H.P. Veluswamy, R. Kumar, P. Linga, Hydrogen storage in clathrate hydrates: Current state of the art and future directions, Appl. Energy 122 (2014) 112–132, https://doi.org/10.1016/j.apenergy.2014.01.063.
[12] Underground Gas Storage in the World – 2023 Status, 2024. https://www.cedigaz.org/underground-gas-storage-in-the-world-2023-status/;.
[13] A.S. Mehr, A.D. Phillips, M.P. Brandon, M.T. Pryce, J.G. Carton, Recent challenges and development of technical and technoeconomic aspects for hydrogen storage, insights at different scales; a state of art review, Int. J. Hydrog. Energy 70 (2024) 786–815, https://doi.org/10.1016/j.ijhydene.2024.05.182.
[14] J. Mouli-Castillo, N. Heinemann, K. Edlmann, Mapping geological hydrogen storage capacity and regional heating demands: An applied UK case study, Appl. Energy 283 (2021), https://doi.org/10.1016/j.apenergy.2020.116348.
[15] Taylor JB, Alderson JE a., Kalyanam KM, Lyle a. B, Phillips L a. Technical and economic assessment of methods for the storage of large quantities of hydrogen. Int. J. Hydrog. Energy 1986;11:5–22. doi:https://doi.org/10.1016/0360-3199(86)90104-7.
[16] A. Ozarslan, Large-scale hydrogen energy storage in salt caverns, Int. J. Hydrog. Energy 37 (2012) 14265–14277, https://doi.org/10.1016/j.ijhydene.2012.07.111.
[17] A.S. Lord, P.H. Kobos, D.J. Borns, Geologic storage of hydrogen: Scaling up to meet city transportation demands, Int. J. Hydrog. Energy 39 (2014) 15570–15582, https://doi.org/10.1016/j.ijhydene.2014.07.121.
[18] HyCAVmobil n.d. https://www.now-gmbh.de/en/projectfinder/hycavmobil-2/ (accessed May 25, 2025).
[19] HyStore n.d. https://hystories.eu/ (accessed May 25, 2025).
[20] Underground Sun Storage 2030″ (USS 2030) n.d. https://www.underground-sun-storage.at/en/ (accessed May 25, 2025).
[21] I. Iordache, D. Schitea, A.V. Gheorghe, M. Iordache, Hydrogen underground storage in Romania, potential directions of development, stakeholders and general aspects, Int. J. Hydrog. Energy 39 (2014) 11071–11081, https://doi.org/10.1016/j.ijhydene.2014.05.067.
[22] Y. Zhang, P.E. Campana, A. Lundblad, J. Yan, Comparative study of hydrogen storage and battery storage in grid connected photovoltaic system: Storage sizing and rule-based operation, Appl. Energy 201 (2017) 397–411, https://doi.org/10.1016/j.apenergy.2017.03.123.
[23] Arthur Cox, Ireland's Climate Action Plan 2023, 2023.
[24] S S. A Comparative Life Cycle Assessment of Hydrogen Production & Storage with Renewable Energy Source and Grid Electricity Source. Journal of Engineering and Applied Sciences Technology 2024:1–5. doi:10.47363/JEAST/2024(6)233.
[25] Rialtas na hÉireann (Government of Ireland), National Hydrogen Strategy, 2023.
[26] IslandMagee Energy. Https://WwwIslandmageeenergyCom/ n.d. https://www.islandmageeenergy.com/ (accessed December 14, 2024).
[27] Caglayan DG, Weber N, Heinrichs HU, Linßen J, Robinius M, Kukla P a., et al. Technical potential of salt caverns for hydrogen storage in Europe. Int. J. Hydrog. Energy 2020;45:6793–805. doi:https://doi.org/10.1016/j.ijhydene.2019.12.161.
[28] J. Gorre, F. Ruoss, H. Karjunen, J. Schaffert, T. Tynjälä, Cost benefits of optimizing hydrogen storage and methanation capacities for power-to-gas plants in dynamic operation, Appl. Energy 257 (2020), https://doi.org/10.1016/j.apenergy.2019.113967.
[29] A. Bejan, G. Tsatsaronis (George), M.J. Moran, Thermal design and optimization, Wiley, 1996.
[30] Wind Stats. Wind Energy Ireland n.d. https://windenergyireland.com/about-wind/the-basics/facts-stats (accessed June 23, 2024).
[31] Cengel YA, Boles MA. Thermodynamics: An Engineering Approach 8th Edition. 2015. doi:https://doi.org/10.1017/CBO9781107415324.004.
[32] A.S. Mehr, A. Moharramian, S. Hossainpour, D.A. Pavlov, Effect of blending hydrogen to biogas fuel driven from anaerobic digestion of wastewater on the performance of a solid oxide fuel cell system, Energy 202 (2020) 117668, https://doi.org/10.1016/j.energy.2020.117668.
[33] L. Lankof, R. Tarkowski, Assessment of the potential for underground hydrogen storage in bedded salt formation, Int. J. Hydrog. Energy 45 (2020) 19479–19492, https://doi.org/10.1016/j.ijhydene.2020.05.024.
[34] M. Guarascio, G.M. Fernandez, In situ testing for rock salt Characterizazion, in: SMRI 1998 Fall Meeting, 1998. Rome, Italy.
[35] Hydrogen Salt Storage Assessment (HYSS) WP3&4 Assessment of salt storage in Irish Sea and Celtic Sea Basins Final Report, 2024.
[36] J. Ślizowski, R. Smulski, S. Nagy, S. Burliga, K. Polański, Tightness of hydrogen storage caverns in salt deposits, AGH Drilling, Oil, Gas 34 (2017) 397, https://doi.org/10.7494/drill.2017.34.2.397.
[37] L. Lankof, K. Urbańczyk, R. Tarkowski, Assessment of the potential for underground hydrogen storage in salt domes, Renew. Sust. Energ. Rev. (2022) 160, https://doi.org/10.1016/j.rser.2022.112309.
[38] K. Zhao, H. Ma, Y. Li, Y. Liu, R. Cai, X. Liang, et al., Stability evaluation of horizontal salt caverns for gas storage in two mining layers: A case study in China, Energies (Basel) 16 (2023), https://doi.org/10.3390/en16217288.
[39] X. Zhang, W. Liu, D. Jiang, W. Qiao, E. Liu, N. Zhang, et al., Investigation on the influences of interlayer contents on stability and usability of energy storage caverns in bedded rock salt, Energy (2021) 231, https://doi.org/10.1016/j.energy.2021.120968.
[40] Z. Liu, L. Lu, L. Ma, H. Luo, X. Yang, M. Babaei, Gas loss prediction in underground hydrogen storage using an improved capacitance–resistance model for carbon neutrality of China, Energy Ecol. Environ. (2025), https://doi.org/10.1007/s40974-025-00356-w.
[41] T.H. Nassan, M. Kirch, M. Amro, Underground hydrogen storage in salt caverns: Laboratory experiments to determine integrity of rock salt and wellbore through effective permeability measurements, Int. J. Hydrog. Energy 99 (2025) 619–631, https://doi.org/10.1016/j.ijhydene.2024.12.105.
[42] Wang J, Wang X, He M, Song Z, Feng S, Liu X, et al. Long-term stability analysis and evaluation of horizontal salt cavern gas storage. J Energy Storage 2023;66. doi: https://doi.org/10.1016/j.est.2023.107413, J Energy Storage.
[43] Li J, Wan J, Liu H, Jurado MJ, He Y, Yuan G, et al. Stability analysis of a typical salt cavern gas storage in the Jintan area of China. Energies (Basel) 2022;15. doi:https://doi.org/10.3390/en15114167.
[44] L. Zhou, Y. Zhou, Determination of compressibility factor and fugacity coefficient of hydrogen in studies of adsorptive storage, Int. J. Hydrog. Energy 26 (2001) 597–601.
[45] Hirscher M. Handbook of hydrogen storage. Top. Appl. Phys. 2010;12.
[46] Groenenberg R, Juez-Larré J, Goncalvez C, Wasch L, Dijkstra H, Wassing B, et al. Techno-Economic Modelling of Large-Scale Energy Storage Systems. 2020.
[47] Jan MICHALSKI, Christopher KUTZ. HyStories: Major results of techno-economic assessment of future scenarios for deployment of underground renewable hydrogen storages. 2022.
[48] A.S. Lord, P.H. Kobos, D.J. Borns, Geologic storage of hydrogen: Scaling up to meet city transportation demands, Int. J. Hydrog. Energy 39 (2014) 15570–15582, https://doi.org/10.1016/j.ijhydene.2014.07.121.
[49] Patonia A, Poudineh R. Cost-Competitive Green Hydrogen: How to Lower the Cost of Electrolysers? n.d.
[50] S.H. Yousefi, R. Groenenberg, J. Koornneef, J. Juez-Larré, M. Shahi, Techno-economic analysis of developing an underground hydrogen storage facility in depleted gas field: A Dutch case study, Int. J. Hydrog. Energy 48 (2023) 28824–28842.
[51] F. Chen, Z. Ma, H. Nasrabadi, B. Chen, M.Z. Saad Mehana, J. Van Wijk, Capacity assessment and cost analysis of geologic storage of hydrogen: A case study in intermountain-west region USA, Int. J. Hydrog. Energy 48 (2023) 9008–9022, https://doi.org/10.1016/j.ijhydene.2022.11.292.
[52] D.G. Caglayan, N. Weber, H.U. Heinrichs, J. Linßen, M. Robinius, P.A. Kukla, et al., Technical potential of salt caverns for hydrogen storage in Europe, Int. J. Hydrog. Energy 45 (2020) 6793–6805, https://doi.org/10.1016/j.ijhydene.2019.12.161.
[53] P. Leone, S. Rory Monaghan, POLITECNICO DI TORINO, Green Hydrogen Hub Development: A Case Study of Galway's Path to a Hydrogen-Powered Future, 2024.
[54] Irish Water business tariff n.d. https://thundersaidenergy.com/downloads/industrial-cooling-chillers-and-evaporators/ (accessed June 16, 2025).
[55] Capping Non-Domestic Connections bills n.d. https://www.water.ie/business/billing/non-domestic-connections (accessed June 16, 2025).
[56] H2Compressor n.d. https://www.man-es.com/process-industry/solutions/compressors-for-hydrogen-applications? (accessed June 17, 2025).
[57] J. Köstlbacher, L. Breuning, F. Nigbur, P. Wienert, D. Khatiwada, Application of an electrolysis system model for techno-economic optimization of hydrogen production in industry-based case studies, Int. J. Hydrog. Energy (2025), https://doi.org/10.1016/j.ijhydene.2025.03.291.
[58] T. Roeder, A. Rosenstiel, N. Monnerie, C. Sattler, Impact of expected cost reduction and lifetime extension of electrolysis stacks on hydrogen production costs, Int. J. Hydrog. Energy (2024), https://doi.org/10.1016/j.ijhydene.2024.08.015.
[59] B.D. James, J.M.M. Nrel, G. Saur, T. Ramsden, Techno-Economic Analysis of PEM Electrolysis for Hydrogen Production, 2014.
[60] D. García-Gusano, K. Espegren, A. Lind, M. Kirkengen, The role of the discount rates in energy systems optimisation models, Renew. Sust. Energ. Rev. 59 (2016) 56–72.
[61] C. Campbell-Stanway, V. Becerra, S. Prabhu, Techno-economic analysis with electrolyser degradation modelling in green hydrogen production scenarios, Int. J. Hydrog. Energy 106 (2025) 80–95, https://doi.org/10.1016/j.ijhydene.2025.01.359.
[62] Cost-effectiveness of Quantitative NMR Applications n.d. https://qnmr.usp.org/t/cost-effectiveness-of-quantitative-nmr-applications/145/1 (accessed June 17, 2025).
[63] Q.V. Dinh, P.H.T. Pereira, V.N. Dinh, A.J. Nagle, P.G. Leahy, Levelised cost of transmission comparison for green hydrogen and ammonia in new-build offshore energy infrastructure: Pipelines, tankers, and HVDC, Int. J. Hydrog. Energy 62 (2024) 684–698, https://doi.org/10.1016/j.ijhydene.2024.03.066.
[64] S.H. Yousefi, R. Groenenberg, J. Koornneef, J. Juez-Larré, M. Shahi, Techno-economic analysis of developing an underground hydrogen storage facility in depleted gas field: A Dutch case study, Int. J. Hydrog. Energy 48 (2023) 28824–28842.
[65] M. Ghaedi, R. Gholami, Characterization and assessment of hydrogen leakage mechanisms in salt caverns, Sci. Rep. 15 (2025), https://doi.org/10.1038/s41598-024-84505-x.